ABSTRACT

Title of Thesis: FRESHWATER SALINIZATION SYNDROME LIMITS MANAGEMENT EFFORTS TO IMPROVE WATER QUALITY

Carly Marcella Maas, Master of Science, 2022

Thesis Directed By: Professor, Dr. Sujay Kushal, Geology

Freshwater Salinization Syndrome (FSS) refers to the interactive effects of salt ions on the degradation of the natural, built, and social systems. FSS can mobilize chemical mixtures, termed ‘chemical cocktails’, in watersheds. The formation of chemical cocktails across space and time depends on the amounts and types of salt pollution, the surrounding land use including conservation and restoration areas, and the location along the flowpath in the watershed. We investigated (1) the formation of

chemical cocktails temporally and spatially and (2) the natural capacity of watersheds and streams to attenuate salt ions along flowpaths with conservation and restoration efforts. We monitored high-frequency temporal and longitudinal spatial chemical changes in stream water in response to different pollution events (i.e., road salt, stormwater runoff, wastewater effluent, and baseflow conditions) and several types of watershed management efforts (i.e., national parks, regional parks, and floodplain reconnection) in six urban watersheds in the Chesapeake Bay region. There were significant relationships between watershed impervious surface cover and mean concentrations of salt ions (Ca^{2+}, K^{+}, Mg^{2+}), metals (Fe, Mn, Sr^{2+}), and nutrients (total dissolved nitrogen) ($p < 0.05$). Principal component analysis (PCA) indicates that chemical cocktails that formed along flowpaths in response to winter road salt applications were enriched in salts and metals (e.g., Na^{+}, Mn, and Cu). During most baseflow and stormflow conditions, chemical cocktails that were less enriched in salt ions and trace metals were attenuated downstream. There was also downstream attenuation of FSS ions during baseflow conditions through management efforts including a regional park, national park, and floodplain restoration. Conversely, chemical cocktails that formed in response to multiple road salt applications or prolonged road salt exposure did not show patterns of attenuation downstream. The spatial patterns were quite variable, with increasing, plateauing, or decreasing patterns based on the magnitude, timing, duration of road salt loading, and extent of management efforts. Our results suggest that FSS can mobilize multiple contaminants along watershed flowpaths, however, the capacity of current watershed management strategies such as restoration and conservation areas to attenuate FSS is limited.

FRESHWATER SALINIZATION SYNDROME LIMITS MANAGEMENT EFFORTS TO IMPROVE WATER QUALITY

by

Carly Marcella Maas

Thesis submitted to the Faculty of the Graduate School of the
University of Maryland, College Park, in partial fulfillment
of the requirements for the degree of
Master of Science
2022

Advisory Committee:
Professor Sujay S. Kaushal, Chair
Professor Karen L. Prestegaard
Dr. Paul M. Mayer

Dedication

To my parents, Andrea and Brian, and brother, Daniel – who have provided unending love, support, and joy. Thank you for always encouraging me to do what is best for myself and to be who I am. I am so thankful to call you not only my family but also my closest friends.

Acknowledgements

I would like to acknowledge my advisor, Dr. Sujay Kaushal for his guidance, support, and countless hours of meetings discussing this project and other interesting research. Thank you also to Dr. Paul Mayer, Dr. Meg Rippy, and Dr. Stan Grant for your assistance in the development of this project. I appreciate all your helpful insight throughout the duration of this research.

I would like also like to thank Christiana Hoff, Joseph Malin, Shantanu Bhide, Lauren Krauss, Peter Vikesland, Kyriaki Papageorou, Robert Stutzke, Phillip Piccoli, Rumya Ravi, Daniel Maas, Janel Niska, Elizabeth Cooper, Daniel Collison, and Allison Dombrowski for help and assistance in fieldwork. Dr. James Webber and Dr. William Anderson, Jr provided thoughtful and constructive reviews of previous drafts. This work was supported by Maryland Sea Grant NA18OAR4170070, NSF Growing Convergence Research Abstract Award #2021089, and the Environmental Protection Agency.

Table of Contents

List of Tables

List of Figures

List of Abbreviations

FSS – Freshwater Salinization Syndrome

ISC – Impervious Surface Cover

UOSA – Upper Occoquan Service Authority

IPR – Indirect Potable Reuse

TDN – Total Dissolved Nitrogen

PCA – Principal Component Analysis

DO – Dissolved Oxygen

Q – Discharge

SC – Specific Conductance

1. Introduction

Freshwater salinization increasingly poses risks to aquatic life, drinking water sources, infrastructure, agriculture, and critical ecosystem services (Kaushal et al., 2005; Iglesias, 2020; Kaushal et al., 2021; Hintz et al., 2022; Kaushal et al., 2022a). The negative impacts of salt ions on natural and built environments are termed Freshwater Salinization Syndrome (FSS) (Kaushal et al., 2018b, 2021, 2022a). Salt ions are the base cations, Na^+, K^+, Ca^{2+}, and Mg^{2+}, and trace metals, such as Cu, Fe, Mn, and Sr^{2+}. Streams affected by FSS are characterized by elevated concentrations of major ions and trace elements from cation exchange, a decrease in biotic richness, increases in eutrophication, and increases in erosion due to sodium dispersion in soils (Canedo-Arguelles et al., 2016; Bird et al., 2018; Kefford, 2018; Behbahani et al., 2021; Kaushal et al., 2021; Szklarek et al., 2022). Global and regional shifts in watershed land use from rural to urban have caused acute and chronic levels of elevated salinity and thereby increased FSS and the potential for the water-quality degradation events (Iglesias, 2020; Kaushal et al., 2022a).

Urbanization and the impervious surface cover (ISC) within a watershed are linked to the effects of FSS (*sensu* Kaushal et al., 2008, 2010, 2014; Moore et al., 2017; Schulz and Cañedo-Argüelles, 2019; Utz et al., 2022). In urban systems, point and nonpoint sources of FSS salt pollution (*e.g.*, discharge, weathering of urban karst (Kaushal and Belt, 2012), road salt, fertilizer, and stormwater runoff) can be transported through the watershed more efficiently along engineered flowpaths

(Kaushal et al., 2005, 2017, 2021; Chen et al., 2018). These point and nonpoint sources of salt pollution have the potential to release chemical cocktails, which are distinct chemical mixtures from a common source that are transported and transformed simultaneously along watershed flowpaths (Kaushal et al., 2018a, 2019, 2020). Chemical cocktails can develop from a variety of anthropogenic sources, including sewage discharge, vehicles, weathering of impervious surfaces, synthetic chemicals, and mineral resources (Bernhardt et al., 2017; Kaushal et al., 2018a, 2018b, 2020; Blaszczak et al., 2019). For example, elevated concentrations of Na^+, Cl^-, SO_4^{2-}, and K^+ can suggest a chemical cocktail of point source sewage and wastewater effluent discharge (Rose, 2007). Nonpoint sources can create distinct chemical cocktails as well, such as road salt runoff and urban stormwater runoff. Road salt pulses can mobilize chemical cocktails of cations (*e.g.*, Ca^{2+}, Na^+, and Mg^{2+}), heavy metals (*e.g.*, Cu, Sr^{2+}, and Mn), and NH_4^+ from soil particles via soil cation exchange (Green and Cresser, 2008; Findlay and Kelly, 2011; Kaushal et al., 2019, 2021; Galella et al., 2021). Stormwater runoff is another issue that degrades the water quality in urban streams, which creates a chemical cocktail of Na^+, Cl^-, HCO_3^-, Ca^{2+}, Mg^{2+}, and Sr^{2+} from the weathering of impervious surfaces (Masoner et al., 2019). In studying multiple elements and nutrients simultaneously along a watershed flowpath using the chemical cocktail approach, we can better infer the transport, transformation, and attenuation capacity of FSS (Kaushal et al., 2018a).

In attempts to improve water quality from nonpoint and point sources of pollution, conservation areas, such as urban parks, and stream-floodplain

reconnection restorations have been implemented in watersheds. These conservation and restoration practices attenuate pollutants by slowing water movement, trapping sediment, increasing nutrient uptake and storage, promoting denitrification, and increasing transpiration (Mayer et al., 2007, 2010; Kaushal et al., 2008b; Tomer et al., 2009). Previous work has found riparian buffers are effective at reducing the concentration of nitrogen in the streams by promoting denitrification in the hyporheic zone and in the floodplain (Lowrance et al., 1997; Sweeney et al., 2004; Mulholland et al., 2008; Vidon et al., 2010; Azizian et al., 2017; Grant et al., 2018). These areas are 'hot spots' of biogeochemical transformations, particularly of denitrification, and nutrient removal, and but can also trap ions to sediments, among other processes (Mayer et al., 2007; Vidon et al., 2010; Kaushal et al., 2020). However, the effects of restoration and stormwater management strategies on the attenuation of salt pollution sources require further investigation (Snodgrass et al., 2017; Kaushal et al., 2022a, 2022b; Galella et al., Accepted). Restored floodplains and wetlands can possibly attenuate salt ions along flowpaths, but there can also be the potential for contaminant mobilization due to ion exchange, changes in pH and solubility, and stimulation of microbial processes (Kaushal et al., 2022a; Galella et al., Accepted). Whether conservation and restoration efforts can attenuate salt pollution sources, similarly to other chemical pollutants, remains an important question in water quality studies.

Although an increase in the scope and magnitude of FSS has been documented over time (Bird et al., 2018; Kaushal et al., 2018b, 2021, 2022a; Bhide et al., 2021; Grant et al., 2022), the natural capacity of watershed flowpaths to retain or dilute FSS

spatially are often less studied. It is also unknown whether the attenuation capacity of a flowpath can be exceeded or saturated under different environmental conditions, such as different pollution events (Maas et al., 2021; Grant et al., 2022; Kaushal et al., 2022a; Galella et al., Accepted). Some salt ions from FSS, such as Na^+, can be attenuated along watershed flowpaths (Kaushal et al., 2022a, 2022b; Galella et al., Accepted), however, there are uncertainties in the distance and extent of the water quality impacts from FSS transmitted downstream. These FSS ions are often transported to sensitive receiving waters, (*e.g.*, major drinking water supplies), and cause damage to infrastructure (Novotny et al., 1998; Kaushal, 2016; Pieper et al., 2018). Further, we do not know if FSS can be mitigated or reversed in any way using restoration and conservation.

In this paper, we investigate how FSS chemical constituents are transmitted or attenuated along watershed flowpaths, across different pollution events, and in response to conservation and restoration efforts. Specifically, we hypothesize that there is a limited capacity for FSS and its water quality impacts to be reversed along hydrologic flowpaths depending upon the amount and timing of salt pollution and conservation and restoration. We propose that watersheds and stream ecosystems can become 'saturated' with salt ions above their natural or engineered attenuation capacity over relatively short time scales in response to certain amounts and types of salt pollution. Whereas most work has focused on understanding changes in salinization over time, our analysis elucidates pathways of ion and contaminant retention and release along watershed flowpaths, including through restoration and

conservation areas. We investigate the transmission and attenuation of FSS in response to three potential sources of FSS pollution: wastewater treatment plant effluent, stormwater runoff, and road salt application, all of which are common forms of pollution in the Mid-Atlantic. Our results can also help identify seasonal and environmental conditions under which chemical cocktails enhanced by salt pollution can be formed, transported, or attenuated in stream water. Results from our work can expand knowledge of riparian buffers and hydrologic systems and help develop principles and paradigms of the mechanisms behind the retention, release, and mobilization of salt ions and other elements, which can then be used to create better management strategies.

2. Materials and Methods

2.1. Study Design: monitoring FSS along watershed flowpaths across space and time

Six watersheds located in Maryland (MD), Washington D.C., and Virginia (VA) were monitored spatially and temporally along watershed flowpaths (Figure 1). Four of the six stream sites have USGS gauges with high-frequency sensors (Table 1) and were sampled every two weeks (Sligo Creek, Paint Branch, Scotts Level Branch, and Anacostia River) to assess the formation of chemical cocktails under various seasonal and weather conditions. Three streams (Scotts Level Branch, Rock Creek, and Bull Run) were sampled longitudinally once a season to characterize spatial changes in water chemistry to evaluate the potential effects of downstream restoration

and conservation areas on attenuating FSS and the potential for salt to saturate attenuation sites along the flowpath. For the longitudinal synoptics' studies, we chose sampling sites on a case-by-case basis to account for site access. The two sampling regimes employed in our study allowed us to explore whether there was a difference in the formation and attenuation of FSS chemical cocktails over a range of weather conditions, seasons, land uses, land management practices, and pollution events.

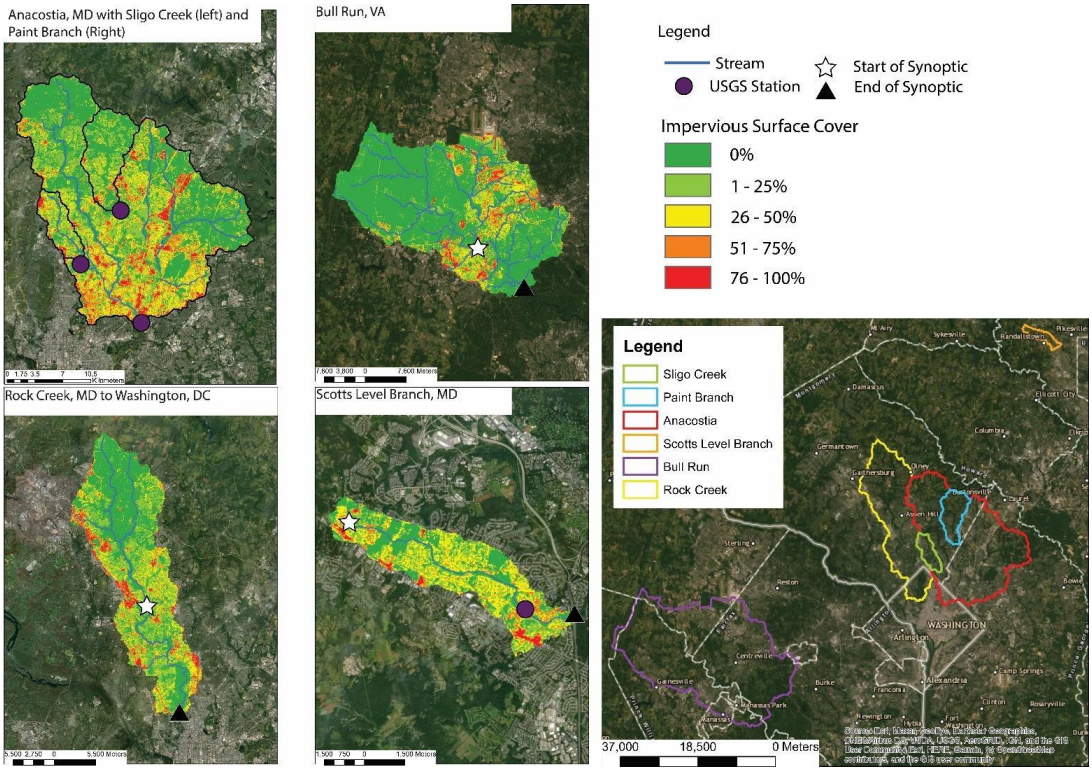

Figure 1. Impervious surface cover of the temporal and spatial monitoring watersheds in the Mid-Atlantic Region of the United States. Green dots indicate the start of the spatial monitoring and red dots indicate the end of the spatial monitoring. Blue stars indicate the USGS monitoring sites, three within the Anacostia watershed and one within the Scotts Level Branch watershed.

Table 1. Watershed and long-term monitoring sensor characteristics for each stream. The latitude and longitude and the watershed characteristics for the temporal monitoring sites, the Anacostia at Bladensburg, Paint Branch, and Sligo Creek, are from the USGS gauge station. The latitude and longitude and the watershed characteristics for the spatial monitoring sites, Scotts Level Branch, Bull Run, and Rock Creek, are from the furthest downstream synoptic sampling point. All sites have specific conductivity and discharge high-frequency sensors except the Anacostia at Bladensburg, which does not have discharge.

Site	**Monitoring Station**	**Latitude, Longitude**	**Drainage Area (km^2)**	**Forest Cover (%)**	**ISC (%)**	**Length of Record**
Anacostia at Bladensburg, MD	USGS 01651007	38.93424, -76.93923	331.5	24.3	30.9	July 2021 to present
Paint Branch, MD	USGS 01649190	39.02972, -76.95067	40.66	27	30.8	October 2007 to present
Sligo Creek, MD	UGSG 01650800	38.98605, -77.00431	16.76	11.9	41.4	October 2008 to present
Scotts Level Branch, MD	USGS 01589290	39.36058, -76.74620	10.41	13.2	39.3	October 2005 to present
Bull Run, VA	Virginia Tech's Occoquan Monitoring Lab	38.72412, -77.38027	502.46	35.67	13	1972 to present
Rock Creek, MD and DC	USGS 01648010	38.90008, -77.05738	198.14	20.4	20.4	April 2007 to present

2.2. Temporal monitoring of water quality in urban streams across land use

Between September 08, 2021 and September 23, 2022, samples were collected twice a month at four USGS gaging stations to analyze stream chemistry over an annual cycle. These sites are the Anacostia River at Bladensburg Waterfront Park (USGS 01651007), Scotts Level Branch at Rockdale, MD (USGS 01589290), Sligo Creek near Takoma Park, MD (USGS 01650800), and Paint Branch near College Park, MD (USGS 01649190) (Table 1), and briefly described below. In addition to stream samples, high frequency data for specific conductivity (SC, in micro-Siemens per centimeter at 25°C), discharge (Q, in cubic feet per second), pH, and temperature (T in °C) were collected from the USGS National Water Information System (U. S. Geological Survey, 2016); the exception was the USGS gauge at Anacostia River at Bladensburg Waterfront Park which did not have discharge recorded at the gauge.

2.2.1. Anacostia Watershed

The Anacostia River is one of the largest tributaries of the Potomac River and drains parts of MD and Washington, D.C. (Velinsky et al., 2011). In this study, three of the temporal monitoring locations lie within the Anacostia Watershed, including two tributaries of the Anacostia River, Paint Branch and Sligo Creek, and downstream on the mainstem of the Anacostia River at Bladensburg, located downstream of these tributaries. The sampling site on the Anacostia at Bladensburg is

tidal with a semidiurnal tide up to 1 m in height (Velinsky et al., 2011). Biological, nutrient, sediment, and bacterial impairment and degradation of the Anacostia caused by regional urbanization has occurred over the past 200 years (Velinsky et al., 2011; Miller et al., 2013). The Bladensburg Waterfront Park site has the largest drainage area of the sites sampled here, and the shortest USGS gauge record and does not have discharge recorded (Table 1). The watershed's geology is sand-gravel facies composed of quartz sand, pebble sand, and silt-clay and silt-clay facies composed of clay with lenses of sand and gravel (Glaser, 2003).

2.2.2. Sligo Creek Watershed

Sligo Creek is a highly urbanized tributary to the Anacostia River near Takoma Park, MD. Our sampling site on Sligo Creek is downstream of numerous stream restorations, including stormwater retrofits, constructed wetlands, channel reconstruction, tree planting, and fish stocking projects implemented in 2001 (Stranko et al., 2012). The bedrock geology is gneiss with quartz, feldspar, mica, and hornblende interbedded with sandstone and mica schist (Froelich, 1975).

2.2.3. Paint Branch

Paint Branch, located near College Park, MD, is a tributary of the Northeast Branch of the Anacostia River. Due to military site restrictions, we sampled 1.5 km upstream of the USGS gauge, which is located between Montgomery and Prince George's County (Miller et al., 2013). Paint Branch is within the alluvium from the

Holocene; however, there are sections of the Laurel Formation upstream, which is a metasedimentary unit of mica gneiss and schist (Glaser, 2003).

2.2.4. Scotts Level Branch

Scotts Level Branch is in Randallstown, MD near Baltimore, MD, and has the smallest drainage area of the sites sampled. The drainage area is residentially developed, with two floodplain reconnection restoration sites along the flowpath (Scotts Level Branch Stream Restoration Project, 2019). Scotts Level Branch crosses two geologic units. Upstream, Scotts Level Branch flows through a medium-grained biotite plagioclase muscovite quartz schist interlayered with a biotite-plagioclase-quartz gneiss. Along the flowpath, a thrust fault shifts the geology to a fine to medium grained amphibolite with pyroxene and chlorite-rich zones (Crowley and Reinhardt, 1980).

2.3. Longitudinal monitoring of stream flowpaths across land use

Three streams, with long-term flow and water quality monitoring network stations, were sampled along the flowpath seasonally. There are different watershed management features along the flowpath at each of the streams, including regional parks, national parks, and stream-floodplain reconnection. To understand the ability of the watershed management features to attenuate FSS chemical constituents, each stream was studied during a baseflow and two road salt events. The sampling conditions during each road salt synoptic is outlined in Supplemental Figure 1. Brief

descriptions of synoptic sampling sites along stream flowpaths are summarized below.

2.3.1. Bull Run (Flowpath from upstream of a Wastewater Treatment Plant through a Regional Park)

Bull Run flows through four regional parks: Manassas National Battlefield Park (20 km^2), Johnny Moore Stream Valley Park (less than 0.005 km^2), Bull Run Regional Park (6 km^2) , and Hemlock Overlook Regional Park (1.6 km^2) (Northern Virginia Regional Park Authority, 2022; Hemlock Overlook Regional Park, 2022; Johnny Moore Stream Valley Park; Manassas and Us). Synoptic sampling began at Bull Run Regional Park and Hemlock Overlook Regional Park. The confluence of Bull Run and a rapidly urbanizing tributary, Cub Run, occurs within Bull Run Regional Park. Cub Run has a higher mean annual storm drainage per surface area with respect to the surrounding area (Dougherty et al., 2007).

The Upper Occoquan Service Authority (UOSA) operates a water reclamation facility which discharges 54 million gallons of treated wastewater effluent per day into Bull Run within Bull Run Regional Park (Onyango et al., 2014). The discharge flows to the Occoquan Reservoir and is part of an indirect potable reuse (IPR) system (Cubas et al., 2014). The UOSA plant includes a conventional treatment, chemical and physical advanced treatment, disinfection, and digestion and sludge handling before discharging to Bull Run (Upper Occoquan Service Authority, 2022). The wastewater treatment plant can remove biological nitrogen, therefore discharging

reclaimed water with lower phosphorus and organic matter concentrations (Cubas et al., 2014). Nitrified effluent is discharged to Bull Run in the warmer months to combat the start of anoxic conditions in the reservoir; in the winter months when the reservoir is oxygenated, UOSA must remove nitrogen in the wastewater and follow regulations for point source nitrogen loads (Cubas et al., 2014).

Four longitudinal synoptic surveys were conducted along the length of Bull Run. Each synoptic included portions of Bull Run above and below the point where treated wastewater is discharged from UOSA. The first two synoptic sampling events were conducted during baseflow conditions and extended from Bull Run Regional Park to the Occoquan Reservoir. The last two synoptics were sampled during snow events (Table 2, SI Figure 1); we were not able to sample the full length of the stream due to safety concerns.

Table 2. Description of each spatial sampling flowpath.

Stream	Date	Longitudinal Distance (km)	Number of Samples Collected	Pollution Pulse Captured
Bull Run	January 13, 2021	16.4	41	Baseflow; denitrification in WWTP; no road salt
	September 17, 2021	15.8	68	Baseflow; rained while sampling; reduced denitrification in WWTP
	January 8, 2022	2.4	20	Road salting event 1; reduced denitrification in WWTP
	January 17, 2022	2.4	20	Road salting event 2; reduced denitrification in WWTP
Rock Creek	February 6, 2021	21.2	25	Road salting event 1
	August 9, 2021	9.2	15	Summer baseflow
	August 13, 2021	20.9	20	Summer baseflow
	September 3, 2021	21.5	5	Urban stormwater; after tropical storm Ida
	January 19, 2022	16	25	Road salting event 2
Scotts Level Branch	March 27, 2021	8.6	12	Spring baseflow
	August 12, 2021	8.6	12	Summer stormwater
	September 2, 2021	8.6	12	Summer stormwater; after tropical storm Ida
	November 2, 2021	8.6	12	Fall baseflow
	January 5, 2022	8.6	12	Road salting event 1
	January 12, 2022	8.6	13	Road salting event 2

2.3.2. Rock Creek (Flowpath from Urban Land Use through Forested National Park)

Rock Creek flows through Rock Creek Regional Park in MD and directly into Rock Creek National Park in Washington, DC. Rock Creek Regional Park, about 7.3 km^2, is managed by the Maryland-National Capital Park and Planning Commission (Montgomery Parks, 2022). The 7.1 km^2 Rock Creek National Park in Washington DC was established in 1890 by the National Parks Service (National Parks Service, 2022). While the river flows through two geographical regions, about 80% of Rock Creek's drainage area is in MD and the remaining 20% in DC (Cintron, 2016). Rock Creek has been the focus of numerous water quality studies over the years, addressing the contribution of the 217 combined sewer outfalls and stormwater drain runoff of pathogens, metals, and organic matter pollution in the stream (Miller et al., 2013; Cintron, 2016).

Five longitudinal synoptic surveys were conducted on Rock Creek, each with varying distances downstream. All synoptics began in Rock Creek Regional Park in Maryland and ended in Rock Creek National Park in Washington, D.C (Table 2).

2.3.3. Scotts Level Branch (Flowpath through Suburban Land Use with Floodplain Reconnection)

Scotts Level Branch is a suburban stream with a narrow riparian buffer (Wood et al., 2022). Two floodplain reconnection projects were completed on Scotts Level Branch (Scotts Level Branch Stream Restoration Project, 2019). The first restoration project at McDonogh Road was completed in the spring of 2014 and 2,000 linear feet

of the stream was restored, starting 2.6 km downstream of the headwaters (Scotts Level Branch Stream Restoration Project, 2019). The second project began in the summer of 2019 at the headwaters, which is a large storm drain, near Marriottsville Road and extended 1,500 feet to Tiverton Road (Scotts Level Branch Stream Restoration Project, 2019). Unlike at Rock Creek and Bull Run, sampling at Scotts Level Branch was conducted at the same location during each synoptic. Samples were collected from the headwaters of Scotts Level Branch at stormwater drain to the confluence of Scotts Level Branch and Gwynns Falls.

2.4. Sample processing and elemental analyses of water samples

All water samples were collected in 125 mL sample bottles that were rinsed in stream water three times prior to sample collection. A Yellow Springs Instrument (YSI) ProQuatro multiparameter meter was used to collect *in-situ* data for temperature, conductivity, pH, dissolved oxygen (DO), and oxidation-reduction potential (ORP). Samples were collected in the mainstem and in the tributaries of the streams when possible. Samples were collected 100 m downstream of the confluence of a tributary and a stream to ensure the sample was well mixed and representative of the stream (Kaushal et al., 2014).

Laboratory methods for sample processing and elemental analyses follow those described previously (standard methods for example, see Haq et al., 2018; Galella et al., 2021; Wood et al., 2022). Each water sample was filtered through a 0.7-micrometer glass fiber filter. Unacidified samples were analyzed on a Total Organic

Carbon Analyzer (TOC-L, Shimadzu, Columbia, MD, USA) for total dissolved nitrogen (TDN). The detection limit for total dissolved nitrogen is 5 μg/mL with a maximum reproducibility coefficient of variance of 1.5% (Shimadzu, 2011). An aliquot of the filtered sample was acidified to 0.5% using ultra-pure nitric acid to prevent flocculation and biological activity. Acidified samples were analyzed via inductively coupled plasma optical emissions spectrometry (ICP-OES) using a Shimadzu Elemental Spectrometer (ICPE-9800, Shimadzu, Columbia, Maryland, USA). The elements analyzed include B, Ba^{2+}, Ca^{2+}, Cu, Fe, K^{+}, Mg^{2+}, Mn, Na^{+}, S^{2-}, Sr^{2+}. The uncertainties for the ICP-OES were 0.6, 10, 0.6, and 0.6 μg/mL for Na^{+}, K^{+}, Ca^{2+}, and Mg^{2+}, respectively (Sellers, 2014).

2.5. Watershed land use characterization along stream flowpaths

The watershed characteristics, including percent forest cover, the percent impervious surface cover, and drainage area was obtained from a 30 m resolution dataset from the 2016 National Land Cover Database using USGS StreamStats web application and ArcMap 10.4. Significant tributaries were identified using StreamStats and Google Maps. Along longer longitudinal profiles, such as Rock Creek and Bull Run, any stream that was named or could be visually identified using StreamStats was considered a major tributary. Any second order stream analyzed via StreamStats was considered a major tributary at Scotts Level Branch. The impervious surface cover and the forest cover in each watershed was obtained from the 2016 National Land Cover Database (U. S. Geological Survey, 2016).

2.6. Statistical analyses

Linear regression relationships were developed between dissolved elemental concentrations in streams, environmental water quality variables (e.g., temperature, dissolved oxygen, discharge, and conductivity) and watershed landscape characteristics. The coefficient of determination of the regression relationships, along with their significance (at $p < 0.05$) were estimated using Excel Regression Analysis.

Principal component analysis (PCA) was used to investigate dominant temporal and spatial parameters across multiple analytes (sensu Helena et al., 2000; Ouyang, 2005; Hu et al., 2013). In this study, we used PCA to investigate the dominant temporal and spatial formation of chemical cocktails using FSS salt ions. PCA was performed on log transformed data, standardized to have a mean of zero and a standard deviation of one. The analysis was conducted in R studio version 1.4 using FactoMineR and factoextra (Lê et al., 2008). A resampling-based stopping rule analogous to the Rand-Lamda rule defined by Peres-Neto et al (2005) was used to identify principal components that explained significantly more variance than expected due to chance at a $p < 0.05$ level (Rippy et al., 2017). Only these components were retained and interpreted in our analysis.

3. Results

3.1. Stream water chemistry changes temporally along a land use gradient

Over the annual cycle, there were seasonal changes in water quality in the salt ions and nutrients (Figure 2, Figure 3). Specific conductance (SC) and salt ion concentrations such as Na^+ peaked sharply during winter months, likely due to road salt applications (Figure 2). Exponential equations were fit to the data from the first salt peak captured by spatial sampling to the return in baseflow conditions from January 5, 2022 to June 3, 2022 (SI Table 1). The Anacostia at Bladensburg, the site in the largest watershed, had a high R^2 indicating an exponential decline occurred in the watershed. Scotts Level Branch, the smallest watershed, had a R^2 of 0.71. Scotts Level Branch was characterized by flashier changes in discharge and specific conductance during road salting events, with specific conductivity peaking at 18000 μS/cm and the Na^+ concentration decreases quicker in a stream after road salt events than larger streams with more sources (SI Table 1).

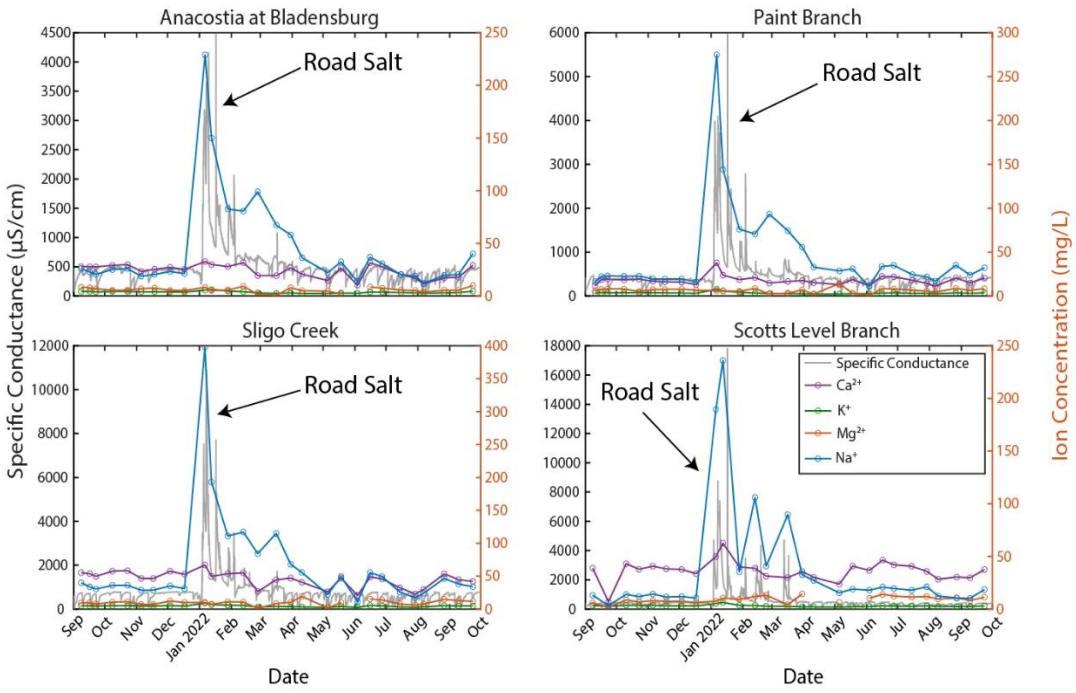

Figure 2. Time series of the temporal monitoring sites and the base cations concentrations (mg/L) plotted with respect to specific conductance. Samples were collected during September 2021- September 2022. The synchronous peak in specific conductance and the ions was due to road salt application.

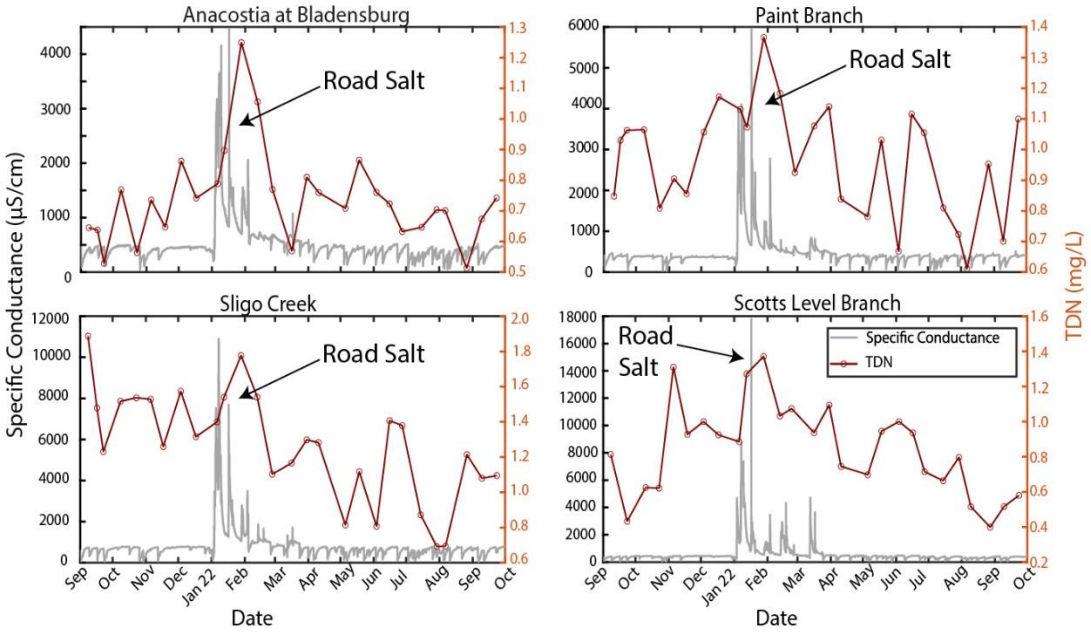

Figure 3. Time series of total dissolved nitrogen (mg/L) with respect to specific conductance.

The total nitrogen concentration in the stream varied seasonally. The highest TDN concentrations were typically sampled following wintertime peaks in specific conductance. Land use significantly influenced the means and ranges of salt ions and nitrogen concentrations in streams across the four watershed sites over an annual cycle (significant correlations summarized in Table 3). There were increases in the concentration of total nitrogen, Ca^{2+}, Fe, K^{+}, Mg^{2+}, Mn, and Sr^{2+} with increasing percent impervious surface cover (ISC) in the watershed (Figure 4), at rates varying between $1.2x10^{-2}$ mg Sr/L/ISC (%) to 2.4 mg Ca/L/ISC (%) ($p < 0.05$). Conversely, there were negative relationships between the salt ion concentrations and the percent forest cover of a watershed, including total nitrogen, Ca^{2+}, Mg^{2+}, and Sr^{2+}, at rates of -$1.6x10^{-2}$, -1.6, -0.25, and -$6.6x10^{-3}$ mg/L/forest cover (%), respectively ($p < 0.0005$).

Redox-sensitive elements, Fe and Mn, were an exception. These elements increased with increasing forest cover at rates of $6.5x10^{-3}$ mg Fe/L/forest cover (%) and $2.1x10^{-3}$ mg Mn/L/forest cover (%). This finding suggests that increased forest cover in a watershed has the increased potential to reduce concentrations of multiple salt ions, metals, and nutrients.

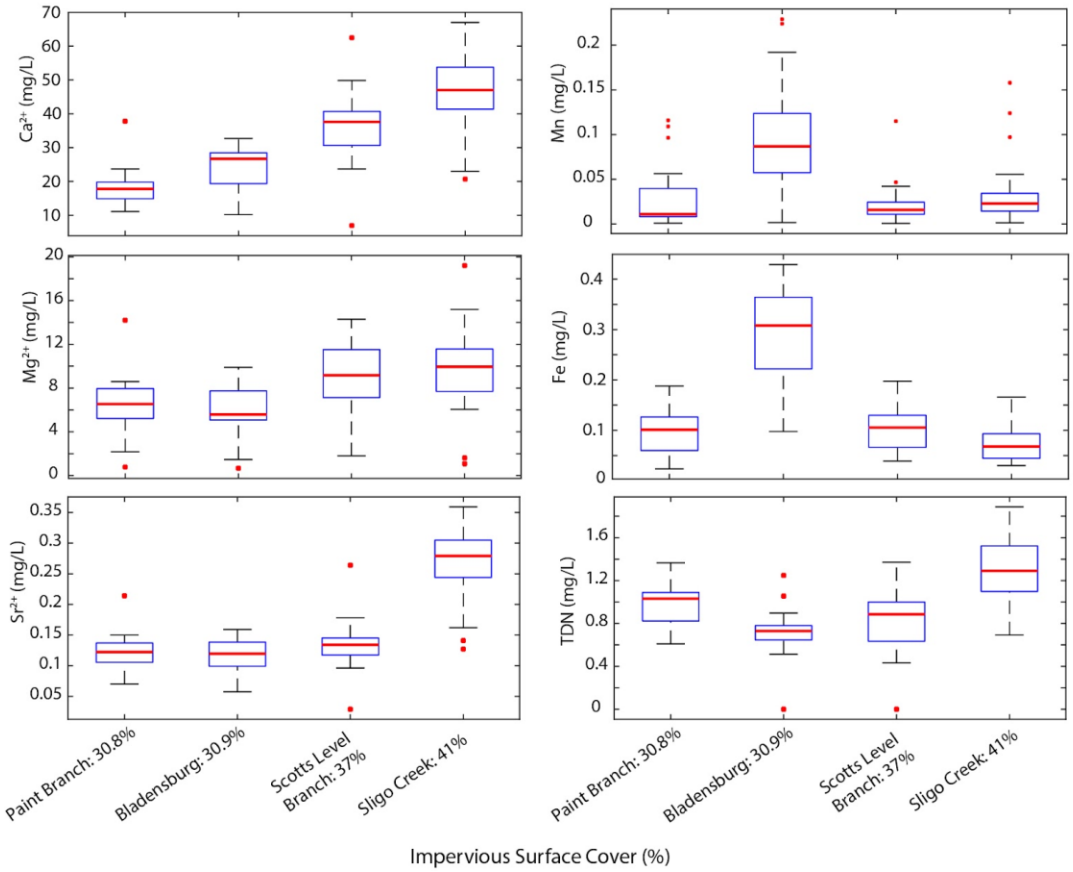

Figure 4. Box and whiskers plot of salt ions concentrations with respect to impervious surface cover percentage in the watershed. These relationships are statistically significant with a p-value of < 0.05. These elements are also statistically significant ($p<0.05$) with respect to the percentage of forest cover within the watershed. n = 111.

Table 3. Linear relationships between field parameters and watershed parameters and ion concentrations. All data is significant with a $p < 0.05$. 2 significant digits are recorded in the table below. Q =Discharge, ISC = Impervious surface cover, SC = specific conductance, SE = Standard Error.

X-Variable	**Ion**	**Equation** y = mx + b	**R^2**	**P-value**	**SE**	**X-Variable**	**Ion**	**Equation** y = mx + b	**R^2**	**P-value**	**SE**
Q (m^3/s)	ORP	84x + 200	0.076	0.020	146	*SC (µS/cm)*	ORP	$-2.4x10^{-2}x + 230$	0.09	0.003	41
	Ca^{2+}	-67x + 42	0.31	$1.23x10^{-7}$	12		Ca^{2+}	$1.4x10^{-2}x + 23$	0.27	$1.4x10^{-8}$	12
	Fe	0.11x + 0.078	0.094	0.007	0.04		Mn	$4.1x10^{-5}x + 0.020$	0.18	0.00002	0.047
	Mg^{2+}	-14x + 10	0.23	0.001	3.1		K^+	$1.9x10^{-3}x + 2.6$	0.60	$7.4x10^{-22}$	0.80
	Sr^{2+}	-0.15x + 0.19	0.06	0.031	0.74		Sr^{2+}	$7.4 \times 10^{-5}x + 0.12$	0.28	$10x10^{-9}$	0.06
ISC (%)	Q	$-1.1x10^{-2}x + 0.53$	0.17	0.00020	0.11		Na^+	0.11x - 18	0.90	$1.7x10^{-53}$	19
	pH	$2.6x10^{-2}x + 6.7$	0.17	0.000010	0.26		TDN	$2.3x10^{-4}x$+ 0.80	0.13	0.00013	0.29
	SC	24x - 250	0.044	0.0317	506		DO	$2.7x10^{-3}x + 7.5$	0.20	0.00010	2.3
	K^+	$6.4x10^{-2}x + 1.4$	0.054	0.014	1.2	*Forest Cover (%)*	Q	$9.7x10^{-3}x - 0.042$	0.30	$1.8x10^{-7}$	0.10
	TDN	$3.4x10^{-2}x - 0.25$	0.22	$1.82x10^{-7}$	0.29		TDN	$-1.6x10^{-2}x + 1.3$	0.11	0.00043	0.29
	Ca^{2+}	2.4x - 52	0.6	$3.78x10^{-23}$	8.8		Ca^{2+}	-1.6x + 62	0.59	$5.0x10^{-23}$	8.8
	Fe	$-1.2x10^{-2}x + 0.55$	0.25	$3.45x10^{-8}$	0.09		Fe	$6.5x10^{-3}x + 0.016$	0.17	0.00001	0.06
	Mg^{2+}	0.36x - 5	0.23	$1.38x10^{-7}$	3.0		Mg^{2+}	-0.25x + 13	0.23	$1. 5x10^{-7}$	3.0
	Mn	$-3.3x10^{-3}x + 0.16$	0.082	0.0042	0.50		Mn	$2.1x10^{-3}x + 0.006$	0.068	0.0094	0.050
	Sr^{2+}	$1.2x10^{-2}x - 0.26$	0.54	$3.7x10^{-20}$	0.049		Sr^{2+}	$-6.6x10^{-3}x + 0.29$	0.36	$3.7x10^{-20}$	0.058

Specific conductance was significantly correlated with multiple elements. Most base cations and trace metals had a significant positive relationship with specific conductance, including Ca^{2+}, K^{+}, Mn, Na^{+}, Sr^{2+}, and total nitrogen. ORP had a negative relationship with specific conductance ($p < 0.003$). Discharge had a negative relationship with Ca^{2+}, Mg^{2+}, and Sr^{2+}, and a positive relationship with redox sensitive elements including Fe ($p < 0.04$).

3.2. Stream water chemical cocktails form seasonally and during different FSS pollution events?

3.2.1. Chemical cocktails are formed seasonally over an annual cycle

The correlation between specific conductance and multiple elements suggests that chemical cocktails are formed and transported in response to FSS (*e.g.*, Kaushal et al., 2018a, 2019; Morel et al., 2020; Galella et al., 2021). PCA was used to diagnose chemical cocktails of salt ions and total nitrogen that formed over an annual monitoring cycle (Figures 2-3). Dimension 1 of the PCA (Figure 5, SI Table 2) captures patterns in salt ions and trace metals (~40% variance explained), whereas dimension 2 of the PCA captures patterns in redox sensitive elements (~21% of the variance explained). Water samples collected during road salt pulses are characterized by elevated concentrations of Na^{+}, K^{+}, Cu, and Mn (see pink circles in the top right quadrant of Figure 5a; small symbols indicate the individual samples, large symbols indicate their central tendency). Most of these ions, except for Cu, have a positive significant relationship with increasing specific conductance (Table 3). Water

samples collected during summer baseflow and stormwater events had lower concentrations of Na^+, K^+, Cu, and Mn (see blue symbols loading opposite the road salt cluster, Figure 5a).

A second chemical cocktail can be seen in the lower right quadrant of Figure 5a, characterized by elevated concentrations of Ca^{2+}, Mg^{2+}, Sr^{2+}, and total nitrogen. These elements had a positive significant relationship with increasing impervious surface cover (Table 3). Stormflow and baseflow samples collected in the fall (brown symbols), spring (green symbols), and summer (blue symbols) had variable concentrations of constituents in these cocktails (note the variability in the locations of samples from these groups with respect to PC dimension 1). Only baseflow and stormflow samples collected in the winter exhibited chemical cocktails that were similar to those evident during road salt events. Notably, you can trace a cycle from one chemical cocktail towards the next by following the seasons, starting with road salt in the upper right quadrant, shifting down and left (away from chemical cocktail 1 as winter transitions to spring and then to summer), relaxing towards chemical cocktail 2 (lower right quadrant) transitioning into fall. The stark differences between chemical cocktails by season illustrate the importance of factoring seasonal changes into our understanding of FSS. Moreover, the significant correlations between different chemical cocktails and variables like land cover (imperviousness) or management practices (road salt application) highlight the importance of these factors as drivers of seasonal change.

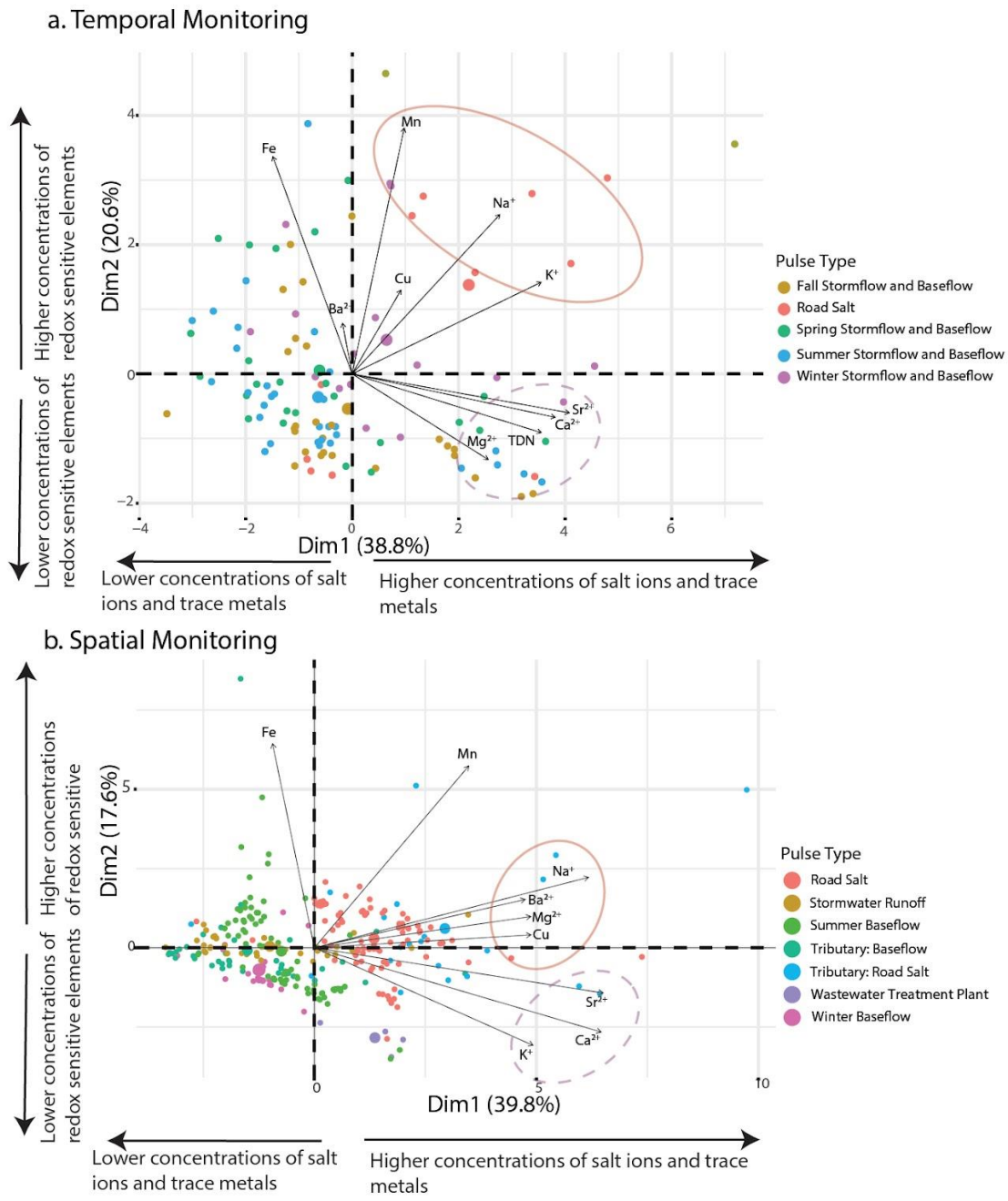

Figure 5. Principal component analysis by pulse type. There is clustering of ions based on the pollution event. The road salt events dominate the PCA on the right-hand side of the plot, as indicated by the circled ions of Na^{+}, Ba, Mg^{2+}, and Cu. The dashed line is a chemical cocktail which could be indicative of urban weathering, composed of K^{+}, Ca^{2+}, and Sr^{2+}.

3.2.2. Chemical cocktails are formed across different FSS pollution events

Distinct chemical cocktails formed spatially following different pollution pulse events. This is evident in Figure 5b, where water samples from particular types of pollutant pulses could be distinguished based on their ion compositions; samples that contained more Na^+, Ba^{2+}, Mg^{2+}, Cu, Sr^{2+}, Ca^{2+}, and K^+ tended to be associated with road salt (red and blue symbols) or wastewater treatment (purple symbols; positive PC dimension 1). Samples that contained less Na^+, Ba^{2+}, Mg^{2+}, Cu, Sr^{2+}, Ca^{2+}, and K^+ tended to be associated with stream baseflow conditions (pink and green symbols) or stormwater runoff (yellow symbols; negative PC dimension 1). Relative to road salt pulses, wastewater pulses were less enriched in Fe and more enriched with Ca^{2+}, Sr^{2+}, and K^+(purple symbols shifted down towards negative PC dimension 2). Summer baseflow samples were enriched in Fe relative to winter baseflow samples, perhaps because Fe was mobilized in the summer during low oxygen conditions (note absence of pink symbols from positive PC dimension 2).

3.3. Chemical cocktails form spatially along watershed flowpaths

Because each stream studied had different longitudinal flowpath lengths, sampling conditions, and surrounding watershed land uses, different chemical cocktails were sometimes evident for different streams. We present a few examples of this below, drawing on the results from three of the streams we sampled, Bull Run, Rock Creek, and Scotts Level Branch. In all streams we evaluated, road salting events dramatically changed the chemical cocktails that were present. This is evident in the

strong loading of samples from road salt events on principal component one (the dominant pattern in ion composition) across all panels of Figure 6 (SI Table 3). This said, distinct chemical cocktails can form across road salt events within the same stream. Baseflow and stormflow chemical cocktails tended to have lower concentrations of salt ions and trace metals than other pulse types. Their composition varies by stream, however, and possibly is a function of impervious surface cover.

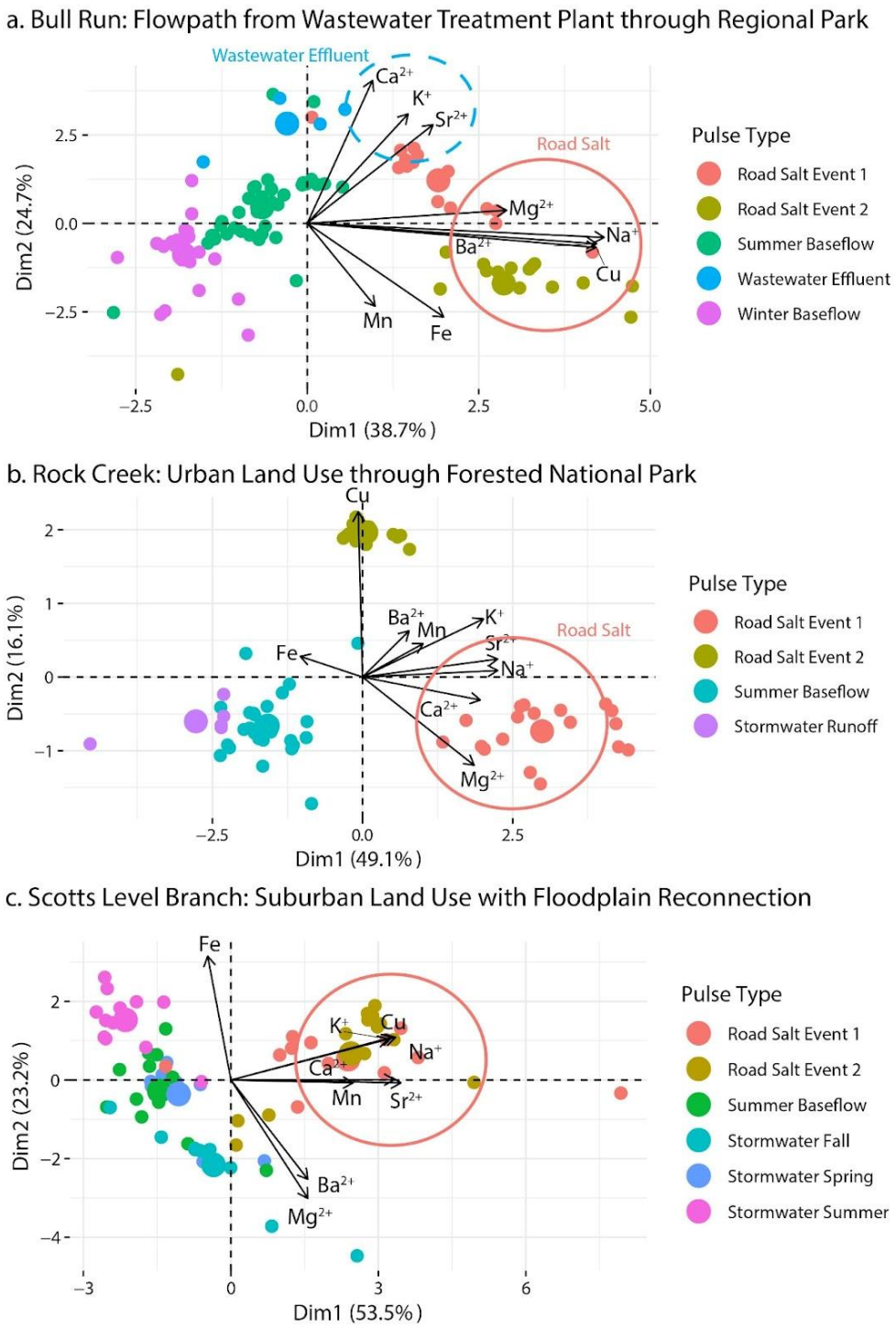

Figure 6. Principal component analysis of each stream sampled for spatial monitoring. The three streams which were monitored longitudinally are analyzed here. In all three synoptics, the road salt chemical cocktails occur on the right side of the biplot. Stormwater and baseflow synoptics are on the left side of the plot, less salt ion enriched.

3.3.1. Chemical cocktails form along flowpath from wastewater treatment plant through regional parks

In Bull Run, different road salting events along the flowpath exhibit different distinct chemical cocktails. Both are elevated in salt ions, however, road salt event 1 was more influenced by Mg^{2+} and Sr^{2+} (Mg^{2+} mobilizes Sr^{2+}) and road salt two was influenced by Na^{+}, Cu, and Ba^{2+} (Na^{+} mobilizes Cu) (Galella et al., 2021).

Water samples collected near and upstream to the wastewater treatment plant have a chemical cocktail characterized by high Ca^{2+}, K^{+}, and Sr^{2+} and low Mn and Fe (blue symbols; positive dimension 2, Figure 6a). Although Na^{+} is a dominant ion in wastewater, individual road salt events increase Na^{+} concentrations in the stream more than wastewater does. This signature aligns with the longitudinal trends in Figure 7 - at the wastewater treatment plant, the in-stream concentrations of K^{+} increased in the stream by an average of 228% and the in-stream Ca^{2+} concentrations increased by an average of 44%. This makes Ca^{2+}, K^{+}, and Sr^{2+} the signature of ions from the wastewater treatment effluent in Bull Run (Jalali et al., 2008). The baseflow samples had low concentrations of all salt ions and trace metals measured. The summer baseflow samples had concentrations that were influenced by the wastewater treatment plant.

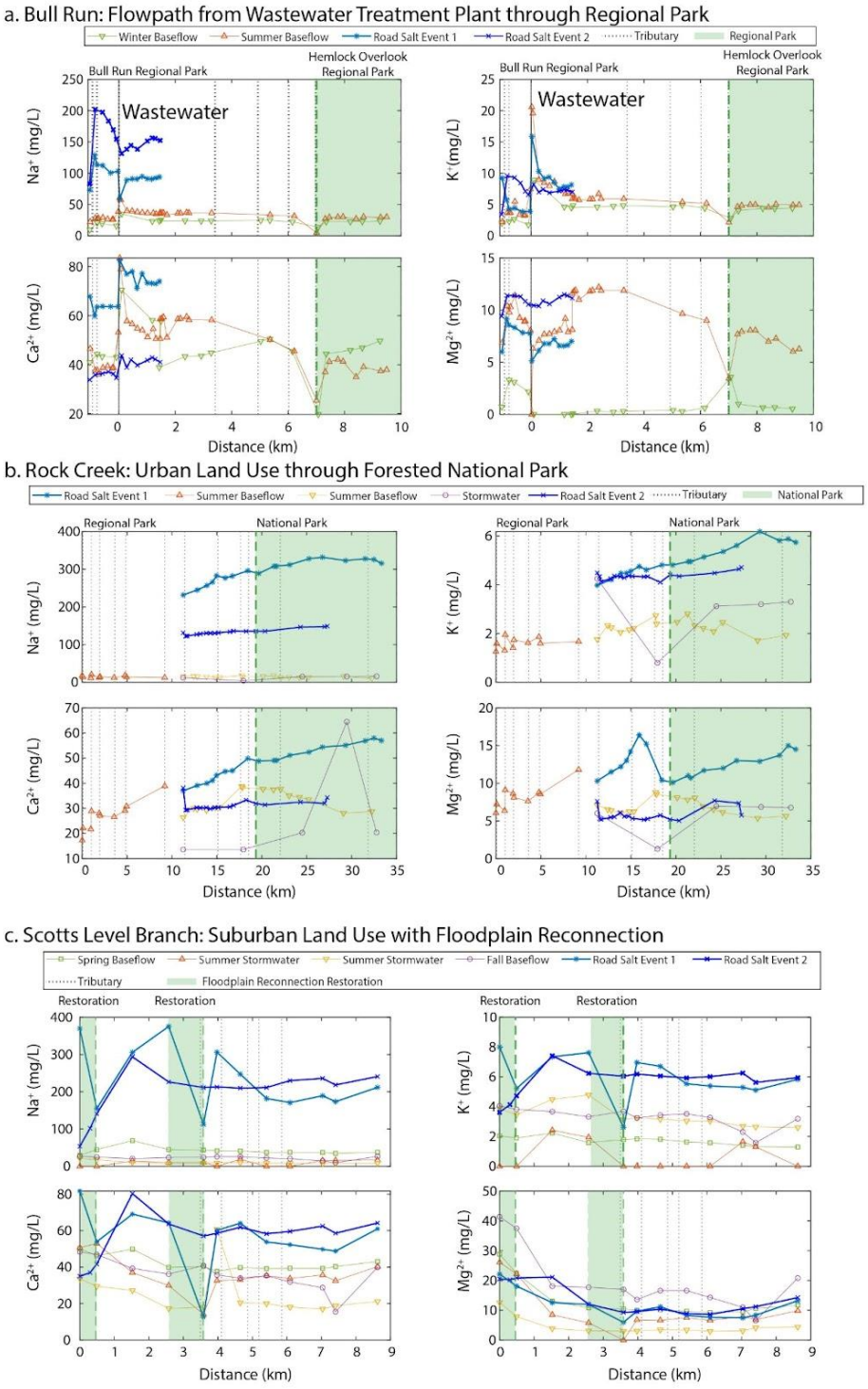

Figure 7. Longitudinal plots of the base cation concentrations vs. distance downstream at the three spatial sampling sites. The green dashed lines indicate either restoration or the transition to conservation. The solid black line in 7a is the wastewater treatment plant effluent which discharges into Bull Run.

3.3.2. Chemical cocktails form along flowpaths from urban land use through forested national park

A stronger divergence between the two road salt events is evident along the flowpath from Rock Creek Regional Park to Rock Creek National Park. The chemical cocktails from road salt event 1 had high concentrations of salt ions, particularly Na^+, Ca^{2+}, and Mg^{2+}, whereas road salt event 2 had higher concentrations of Cu (Figure 6b). These differences are likely due to the conditions during the road salting event. Road salt event 1 was sampled four days after a snow event (SI Figure 1). During that snow event, the stream's conductivity at the USGS gauge in Rock Creek National Park peaked around 11,700 µS/cm with a discharge of 1.9 ft^3/s (SI Figure 2). The second road salt event was collected 3 days after a smaller snowstorm (peak specific conductance of 6,230 µS/cm, discharge of 10.5 ft^3/s), which may have transmitted salt ions (K^+, Na^+, Ca^{2+}, Mg^{2+}) out of the watershed more quickly. During baseflow, Rock Creek exhibited stormwater and baseflow samples with elevated ion concentrations, in particular Fe (Figure 6b).

3.3.3. Chemical cocktails form along flowpaths suburban land use with floodplain reconnection

The composition of the baseflow and stormwater flow chemical cocktails depended on the impervious surface cover in the watershed. Scotts Level Branch (Figure 6c) has the highest impervious surface cover as well as the smallest watershed area. The stormwater and baseflow events grouped on the biplot by the seasons,

though all were elevated in salt ions. In contrast to the other two streams, both road salt events at Scotts Level Branch were associated with similar chemical cocktails, containing high concentrations of a highly correlated chemical cocktail of Cu, Na^+, K^+, Ca^{2+}, Mn, and Sr^{2+}. The summer stormwater and summer baseflow events were correlated with chemical cocktails heavily elevated in Fe. During the stormwater events in the spring and the fall, the chemical cocktail was elevated in both salt ions and Fe.

3.4. Attenuation of chemical cocktails along flowpaths across different hydrologic conditions

Chemical cocktails are formed and can be attenuated along flowpaths, but these patterns depend on the dominant pollutant type, season, land use, and location within the watershed. In many cases, there was downstream attenuation of nutrients, major ions, and trace metals with distance downstream, particularly during baseflow and stormwater flow events. However, the patterns of attenuation depended strongly on hydrologic conditions and seasonality. Tributaries of the streams studied are indicated by black dashed vertical lines in Figure 6. We discuss a few examples of patterns of longitudinal attenuation of chemical cocktails below.

3.4.1. Chemical cocktails are attenuated along longitudinal flowpaths in regional parks

During winter baseflow and summer baseflow at Bull Run, there was an increase in concentration of Ca^{2+}, K^+, and Na^+ due to the wastewater effluent which then

decreased in concentration downstream throughout the regional park (Figure 7a). Mg^{2+} showed an increasing pattern longitudinally throughout the regional parks. The rapid decline by the second regional park, indicated by the green dashed line and the highlighted green box, is from the confluence of Bull Run and a large tributary, Popes Head Creek.

An increase in the concentration of Na^{+}, K^{+}, and Mg^{2+} was observed during the road salt events. The peak in concentrations of salt ions was from a highly urbanized tributary, Cub Run. For both road salt events, Na^{+} and Mg^{2+} peaked at the confluence of Cub Run and Bull Run. The concentration then declined to the wastewater treatment plant, afterwards increasing through the flowpath. A similar pattern occurred for Ca^{2+} and K^{+} during the second road salt event, although both ions increased in concentration at the wastewater treatment plant due to effluent.

3.4.2. Chemical cocktails are attenuated from urban land use through forested national park

Patterns of attenuation of the salt ions were observed during summer baseflow within the Rock Creek National Park (Figure 7b). The concentrations of the salt ions increased during the regional park and decreased in the national park. The road salt events showed different attenuation throughout the longitudinal flowpath amongst the streams or the two road salt events. There were changes in discharge and specific conductance over the road salt pulse (Supplementary Figure 2). During the road salt events, there were increasing concentrations for all salt ions. While Ca^{2+}, K^{+}, and Na^{+}

increased incrementally throughout the flowpath, Mg^{2+} was more variable. The concentration of Mg^{2+} increased until approximately 16 km downstream of the headwaters, rapidly declined, and then increased throughout the national park. Within Rock Creek National Park, the concentrations of salt ions all decreased along the flowpath. Along the Rock Creek flowpath, the base cations showed trends of decreasing concentrations at the site before the national park, perhaps due to dilution from a tributary above stream. Within the National Park, there are increasing trends in concentration which attenuate in the park at 25 km downstream.

3.4.3. Chemical cocktails are attenuated along suburban land use with floodplain reconnection

Similar patterns of attenuation were observed along the flowpath through the residential area with restoration at Scotts Level Branch (Figure 7c). There were patterns of downstream attenuation for the salt ions during the baseflow events. In Scotts Level Branch, baseflow ion concentrations were lower at the downstream end of the restoration areas compared to the upstream concentrations. However, during baseflow, the restoration areas were a source of K^{+}. Two stormwater events were captured at Scotts Level Branch, one of which was after tropical storm Ida. The monovalent salt ions increased between the first and second restoration site. The divalent base cations concentration decreased along the length of the synoptic. Ca^{2+} did not show a pattern of decline after the second restoration.

At Scotts Level Branch, the two road salt events differed at the restoration sites. During the first road salt event, the restoration sites acted as a sink for salt ions. The concentrations, in general, decreased throughout the restoration sites and along the length of the flowpath. However, during the second road salt event, these restoration sites acted as a source of the salt ions. There was increasing concentrations or plateauing of the concentrations at the floodplain restoration sites. At Scotts Level Branch, salt ion concentrations decreased through the restoration areas during the first road salt event sampled (Figure 7) and the restoration area acted as a sink. Nevertheless, these restoration areas acted as a source for the base cations during the second road salt event, sampled just one week later. In these reaches, the ion concentration increased, plateaued, or only slightly declined. The restoration became overwhelmed by the excess road salt and was unable to provide water quality improvements.

3.5. Effects of riparian buffer width on attenuation of different chemical cocktails

The riparian buffer width and percent forest coverage was calculated at each spatial sampling location for each season (Figure 8). The trends in percent forest differs from the riparian buffer width. At Bull Run, both the riparian buffer width and the percent forest increase in the second regional park. This pattern did not hold true at Rock Creek and Scotts Level Branch. At Rock Creek, the riparian buffer width increases throughout the national park, even though the percent forest increases

because the land use surrounding Rock Creek Park becomes more urban along the flowpath. Above the national park, the land use is exurban suburban and predominantly urban sprawl from Washington, D.C. In Washington, D.C., the land use surrounding the national park is intensely urban. Although there is a larger riparian buffer width, the remaining areas within the watershed are not forested. Scotts Level Branch is surrounded by suburban land use, with residential homes on either side of the stream. There is an increase in the forest percentage between the restoration areas due to the replanting of native vegetation. However, sampling was conducted at the end of the restoration to assess the changes in chemistry between the upstream impaired waters and after the restoration, so this was not captured in the riparian buffer width.

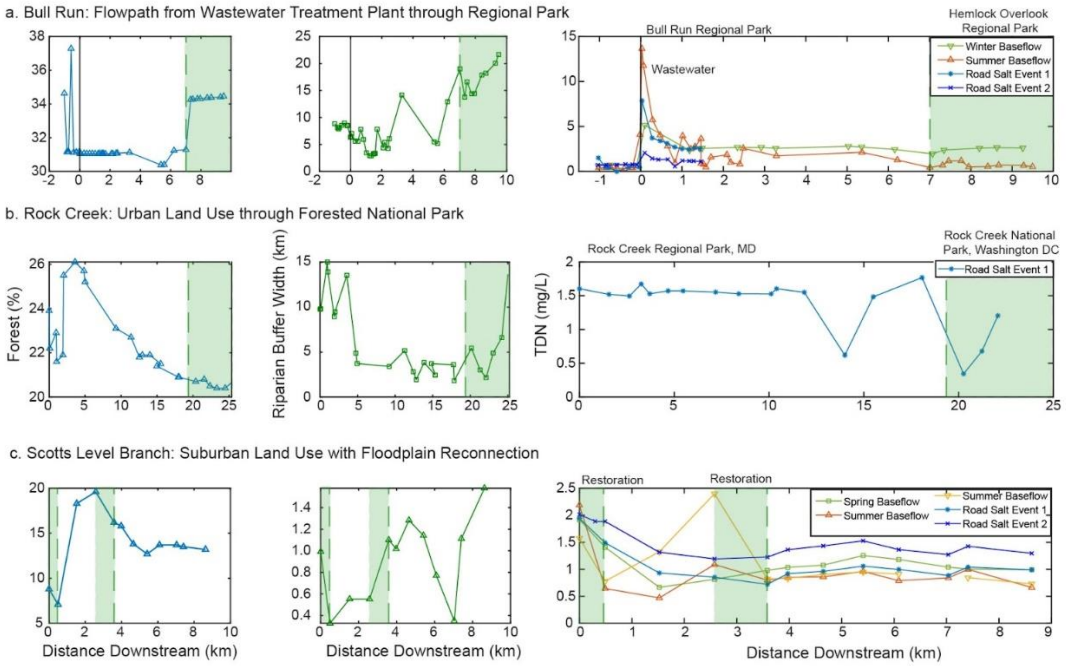

Figure 8. Percent forest within the watershed, riparian buffer width, and concentration of total dissolved nitrogen with distance downstream for each spatial sampling site.

Nitrogen concentrations increase at the wastewater treatment plant and decline downstream with increasing forest cover and riparian buffer width in the watershed at Bull Run (Figure 8a). In Rock Creek National Park, nitrogen concentrations remain elevated and fluctuate during road salt events (Fig. 8b). However, Scotts Level Branch, a restored site where the headwaters (Figure 8c) are a large stormwater culvert which drains to a floodplain restoration area, had high concentrations of N which declined through the first restoration and along the sampling event.

P-values were assessed for the linear regressions between the riparian buffer width and 11 different ions (B, Ba^{2+}, Ca^{2+}, Cu, Fe, K^{+}, Mg^{2+}, Mn, Na^{+}, S, Sr^{2+}) at all spatial sampling sites. TDN was analyzed at Bull Run for the summer and winter

baseflow, but the relationships were not statistically significant, with p-values of 0.077 during the summer baseflow and 0.67 in the winter baseflow. There were significant relationships for Bull Run during the winter and summer baseflow events and Rock Creek during the road salt events ($p < 0.05$) (Figure 9a and 9b, Table 4). During the Bull Run synoptic period during the winter months, two of the twelve ions have decreasing concentrations with increasing km of riparian buffer width: B and S with slopes of $-6x10^{-3}$ and $-8.9x10^{-3}$ (mg/L)/km respectively. However, during the summer synoptic at Bull Run, six of the twelve ions analyzed showed attenuation along the longitudinal flowpath. These ions include B, Ba^{2+}, Ca^{2+}, Mg^{2+}, Na^{+}, and Sr^{2+}. These ions have slopes ranging from -4.8 (mg Ca^{2+}/L)/km to -8.1x10 Only B had significant negative relationship between the winter and summer baseflow synoptic, although these slopes are not statistically significant from each other.

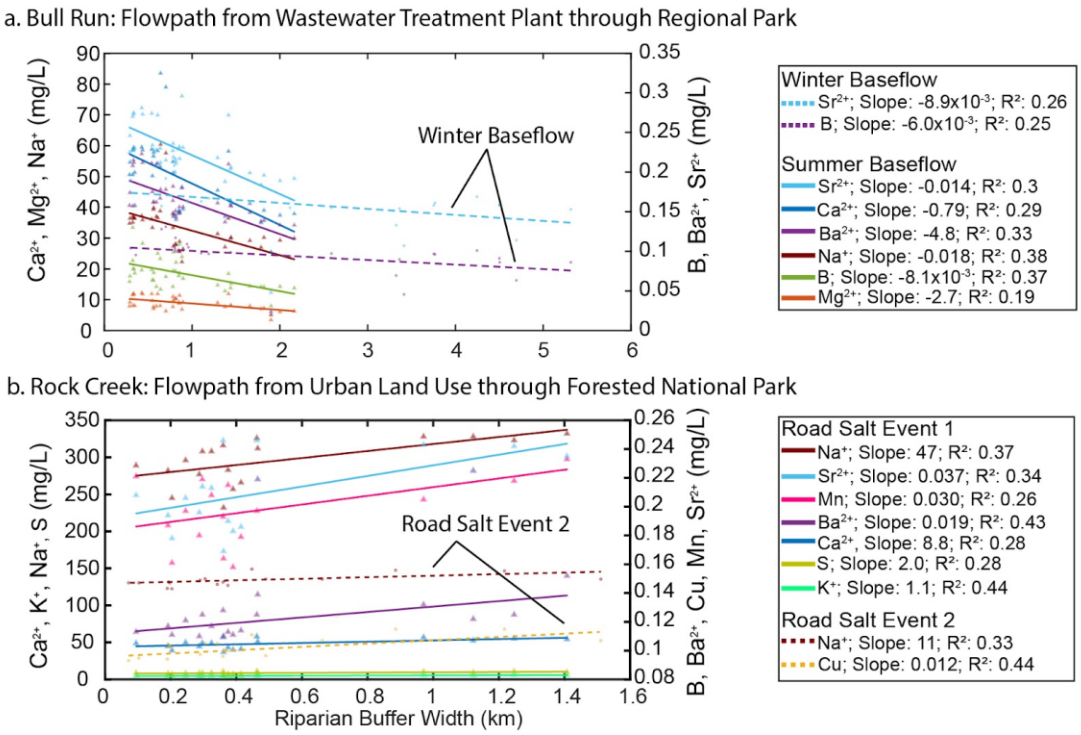

Figure 9. Significant relationships between the riparian buffer width and different ions at all the spatial sampling sites. The top plot is at Bull Run and the bottom plot is at Rock Creek. There were no significant relationships at Scotts Level Branch between ion concentrations and the riparian buffer width.

At Rock Creek, statistically significant relationships between riparian buffer width and ions occurred during road salt events ($p < 0.05$). The first road salt event, characterized by higher specific conductance and discharges, had seven ions which were positively significantly related to riparian buffer width. These ions are Ba^{2+}, Ca^{2+}, K^{+}, Mn Na^{+}, S, and Sr^{2+}, all with p-values less than 0.035. The base cations, such as Na^{+}, Ca^{2+}, K^{+} had high rates of change per kilometer, such as 47, 8.8, and 1.1 (mg/L)/km. During the second road salt event with the lower specific conductance and discharge the statistically significant relationships were of Cu and Na^{+}, with

slopes of 0.012 and 11 (mg/L)/km, respectively. The slopes of Na^+ are statistically significant from one another (Table 4).

Table 4. Linear mathematical relationships between the ions and riparian buffer width (m) along the longitudinal sampling sites. All of the data are significant with a p-value < 0.05. 2 significant figures are reported. SE = Standard Error.

Bull Run						**Rock Creek**					
Season	Ion	Regression Equation	R^2	p-value	SE	Road Salt Event	Ion	Regression Equation	R^2	p-value	SE
Winter	B	$y = -6x10^{-3}x + 0.11$	0.25	0.02	0.015	*Event 1*	Ba^{2+}	$y = 0.019x + 0.11$	0.43	0.003	0.0088
	Sr^{2+}	$y = -8.9\ x10^{-3}x + 0.19$	0.26	0.027	0.022		Ca^{2+}	$y = 8.8x + 44$	0.28	0.026	5.8
Summer	B	$y = -8.1x10^{-3}x + 0.08$	0.37	$1.1x10^{-4}$	0.030		K^+	$y = 1.1x + 4.5$	0.44	0.003	0.49
	Ba^{2+}	$y = -4.8x + 56$	0.33	$1.5x10^{-4}$	0.016		Mn	$y = 0.030x + 0.18$	0.26	0.031	0.021
	Ca^{2+}	$y = -0.79x + 10$	0.29	$5.5x10^{-4}$	9.9		Na^+	$y = 47x + 270$	0.37	0.008	25
	Mg^{2+}	$y = -2.7x + 37$	0.19	$5.5x10^{-3}$	1.8		S	$y = 2x + 7.8$	0.28	0.023	1.3
	Na^+	$y = -0.018x + 0.25$	0.38	$3.0x10^{-5}$	8.0		Sr^{2+}	$y = 0.037x + 0.19$	0.34	0.012	0.021
	Sr^{2+}	$y = -0.014x + 0.19$	0.30	$2.7x10^{-4}$	0.033	*Event 2*	Cu	$y = 0.012x + 0.10$	0.44	0.003	0.0053
							Na^+	$y = 11x + 130$	0.33	0.016	6.5

4. Discussion

Overall, the formation and attenuation of FSS chemical cocktails across space and time in watersheds due to: (1) amounts and types of salt inputs, (2) differences in surrounding land use, conservation, and restoration, and (3) location within the watershed. FSS manifests itself in diverse forms and can mobilize different chemical cocktails based on pollution sources (*e.g.,* sewage, urban runoff, and road salt). FSS chemical cocktails show different patterns of attenuation downstream based on pollution sources, and we found that can be the potential for conservation and restoration areas to reduce water quality impacts of FSS. In the following section we discuss patterns in propagation and attenuation of FSS chemical cocktails, the role of riparian conservation and restoration areas in attenuation of FSS, and the potential for salt saturation along flowpaths.

4.1. Formation and attenuation of treated wastewater chemical cocktails across time and space

Treated wastewater formed a unique, distinct chemical cocktail of Ca^{2+}, K^{2+}, and Sr^{2+} (Figure 6a) in this study. During baseflow events, the concentrations of Na^{+}, Ca^{2+}, and K^{+} increased at the wastewater treatment plant while Mg^{2+} declined (Figure 7a). The most common ions in wastewater in general include total nitrogen, K^{+}, Na^{+}, Cl^{-}, and SO_4^{-2} with Mn, Ni^{2+}, Zn^{2+}, Cr, Cu, As, Pb, Cd^{2+} (Kaushal et al., 2020). A study along Bull Run found that 64% of the Na^{+} sources in the effluent from the

wastewater treatment plant were unknown (Bhide et al., 2021). While Na^+ is typically a dominant ion in treated wastewater effluent, the excess of Na^+ from the road salt events causes Ca^{2+} and K^+ to be a unique overwhelming signature from the effluent. Although not measured in this study, wastewater also is a source of nutrients, organic matter, emergent pollutants, and pathogens to streams (Castelar et al., 2022), all of which can create chemical cocktails that can be transported and transformed along a flowpath.

The summer baseflow chemical cocktails found at Bull Run were most similar to wastewater effluent during the low flow conditions, indicating that the wastewater treatment plant was a large contributor to the discharge. Across the contiguous US, wastewater is estimated to contribute to over 50% of the flow in 900 streams and during the summer the treated effluent can account for up to 100% of the downstream discharge (Ribot et al., 2012; Rice and Westerhoff, 2017). In water-stressed urban regions, streams become dependent on wastewater during baseflow, which alters the hydrologic nature of intermittent to perennial streams in arid climates (Luthy et al., 2015; Castelar et al., 2022).

Indirect potable reuse is a sustainable management practice which discharges highly treated wastewater to the surface water and the groundwater that can, in turn, be used as a drinking water source for a community downstream (Rodriguez et al., 2009). The wastewater treatment plant discharges effluent into Bull Run as surface water recharge which flows to the Occoquan Reservoir, which is used as the receiving waters for the Fairfax Country Griffith drinking water plant (Onyango et al., 2014).

Therefore, the watershed management system is established upon the ability for Bull Run to attenuate the additional nutrients and ions, particularly total nitrogen. A stream's ability to longitudinally biogeochemically process and attenuate these nutrients and ions from the wastewater treatment plant is dependent on the flow conditions, residence times of the ions, and seasonality (Castelar et al., 2022).

Depending on the pollutant and the discharge, the stream can act as a source, sink, or transporter downstream of the wastewater treatment plant. Overall, Na^+, K^+, and Ca^{2+} were attenuated throughout the entire study reach after the wastewater treatment plant during baseflow. Mg^{2+} showed different patterns – there were increasing patterns before the wastewater treatment plant which declined at the effluent and along the flowpath. Future work should continue to investigate the transport and biogeochemical transformation of various pollutants and contaminants before and after wastewater effluent enters streams.

4.2. Formation and attenuation of road salt chemical cocktails along flowpaths

Chemical cocktails formed from road salt pollution in urban waterways created salt ion-enriched chemical cocktails. In general, these chemical cocktails were dominated by high correlations between salt ions, such as Na^+, and co-mobilized trace metals, including Cu (Figure 5a, Figure 5b). However, the elemental composition of the road salt chemical cocktails varied by location – Bull Run was dominated by Na^+, Mg^{2+}, Cu, and Ba, Rock Creek had two distinct chemical cocktails with Na^+, Ca^{2+},

and Mg^{2+} dominating one road salt event and the other was driven by Cu, and Scotts Level Branch had a chemical cocktail of Na^{+}, Ca^{2+}, K^{+}, Mn, Sr^{2+}, and Cu.

The influx of salt ions into the surface water from road salts increases the base cation exchange and the mobilization of trace metals in sediments and soils (Findlay and Kelly, 2011; Galella et al., 2021). The dominant cation in road salt, Na^{+}, has a large radius and a high charge with respect to other monovalent cations (Findlay and Kelly, 2011). Therefore, Na^{+} is very effective at competing for negatively charged sites on clay soil particles and displaces other adsorbed ions including Ca^{2+}, K^{+}, Mg^{2+}, Pb, Cu, Mn, and Sr^{2+} (Findlay and Kelly, 2011; Galella et al., 2021). However, if different types of road salts are applied (*i.e.*, $CaCl_2$ or $MgCl_2$), there is the potential for distinct chemical cocktails (Kaushal et al., 2019; Galella et al., 2021). These divalent cations have the capacity for greater cation exchange rates on soil particles; Mg^{2+} displaces Cu while Ca^{2+} displaces Zn, Pb, and Cd^{2+}, which are eventually transported into the surface water (Kaushal et al., 2019; Galella et al., 2021).

The differences among the formation of salt ion-enriched chemical cocktails from road salt events could depend on the timing and intensity (*i.e.*, the quantity of road salt application per impervious surface cover) of road salt application and the sampling event within the watershed. The composition of road salt chemical cocktails can vary temporally throughout an episodic salinization event caused by road salt application (Haq et al., 2018; Galella et al., 2021). As the specific conductivity rises and peaks from the influx of road salt, there is a strong relationship between the base cations and the trace metals (Galella et al., 2021). This relationship suggests

comobilization of trace metals due to cation exchange during road salt events (Kaushal et al., 2019, 2021; Galella et al., 2021). After the initial peak in road salt pulse, the declining specific conductance suggests a weaker relationship between the base cations and trace metals (Galella et al., 2021). In our results, we observed trace metal comobilization with base cations during road salt events both temporally and longitudinally (Figures 7). However, there were also different chemical cocktails that may have also formed based on the longitudinal stream characteristics, surrounding land use, and conservation and restoration throughout the stream network.

During road salt events, there were not downstream patterns of attenuation along the flowpath, even within conservation and restoration. Through Bull Run Regional Park, Rock Creek Regional and National Park, and the restoration sites along Scotts Level Branch, there were variable patterns of retention and release with Na^{+}, Ca^{2+}, Mg^{2+}, and K^{+} (Figure 7).

4.3. Formation and attenuation of chemical cocktails from stormwater runoff across time and space

Stormwater runoff and baseflow conditions formed chemical cocktails less enriched in salt ions and trace metals with respect to road salt chemical cocktails. The stormwater runoff events are generally shorter in length than winter stormwater events generally, and the influence of corrosion releasing heavy metals decreases (Hallberg et al., 2007). Many of the samples were collected on the receding limb of the hydrograph, a few days after a stormwater event and therefore not capturing the

"first flush" of pollutants (Kayhanian et al., 2012). The most pollutants and heat from impervious surfaces enter the stream during the first portion of the stormwater runoff event than the remainder of the event (Kayhanian et al., 2012; Blaszczak et al., 2019).

There were still spatial and temporal patterns which emerged during baseflow and stormflow. During winter baseflow events (Figure 5a), the chemical cocktail is influenced by ions such as Mn, Na^+, K^+, and Cu, which are dominant in the road salt chemical cocktail. The remaining three months are grouped close together (Figure 5a, 5b) as chemical cocktails which are both less enriched in salt ions and redox sensitive ions than the road salt chemical cocktail. At Rock Creek and Scotts Level Branch, the summer baseflow and stormwater runoff both had higher concentrations of Fe than during road salt conditions. Fe is sourced from the watershed and, in general, is associated with increases in dissolved organic matter and reducing conditions (Figure 6b, 6c) (Ekström et al., 2016). Stormwater runoff chemical cocktails are more challenging to quantify and characterize due to the diffuse sources, including soil erosion, vehicles, human and animal waste, fertilizers, household chemicals, industrial processes, atmospheric fallout, and paints and preservatives (Aryal et al., 2010). Common inorganic ions in urban stormwater runoff include heavy metals, such as Pb, Cr, Zn^{2+}, Cu, Ni^{2+}, and Cd^{2+} generally associated with finer sediment fraction runoff (Aryal et al., 2010).

4.4. Roles of conservation and restoration in the attenuation of chemical cocktails, salt saturation, and limitations in response to Freshwater Salinization Syndrome (FSS)

Conservation and restoration areas are implemented in impaired watersheds to reduce the concentration of nutrients such as nitrogen through denitrification (Mayer et al., 2007). However, these areas have the potential to attenuate transport of salt pollution further downstream when the rates of watershed salt loading are lower such as during baseflow and stormflow events, however, the effects are variable during road salt events. There were patterns of increase, plateau, and decline along a flowpath, depending on the surrounding watershed characteristics. There were patterns of increase with all the salt ions in parks at Bull Run and Rock Creek (Figure 7a, 7b). In the floodplain reconnection at Scotts Level Branch, the restoration acted as a sink during the first road salt event and a source of ions during the second road salt event (Figure 7c). These green spaces, such as urban forests and restorations, benefit urban streams by reducing pollutant concentrations in urban runoff (Livesley et al., 2016). In comparison to impervious surfaces, trees and vegetated areas can intercept more rainfall, have higher infiltration rates into soils, and reduce runoff during stormwater events (Nowak, 2006).

Previous research suggested nitrogen can be effectively removed by riparian buffers (Mayer et al., 2007). Wider riparian buffers provide more area for root uptake of nitrogen and favor denitrification (Mayer et al., 2007). At Bull Run along the flowpath from the wastewater treatment plant through the regional parks, there were

no significant patterns between riparian buffer width and total nitrogen concentrations during the summer or winter baseflow. This could be due to the vegetation type, root zone depth, or hydrological flowpath (Mayer et al., 2007). However, during baseflow events, there are some significant patterns of decreasing ion concentration with increased riparian buffer width. In the summer and early fall, there are warmer surface water temperatures, more direct sunlight, and higher autotrophic uptake in the stream causing higher primary productivity (Ledford et al., 2017). Therefore, there is the potential for attenuation of ions with increased riparian buffer width. However, during road salt events, there are positive relationships. At Rock Creek, the riparian buffer width increases at the end of the flowpath in Washington DC. Many of the ions increased with increasing riparian buffer width, indicating that the riparian buffer was overwhelmed and saturated from FSS ions.

Recent work suggests there can be retention of the salt ions along floodplains in soils across the year (Ledford et al., 2016; Maas et al., 2021). Salt ions accumulate in the sediments and groundwater, resulting in elevated salt ion and trace metal concentrations several months after the specific conductance and Na^+ concentration decline (Cooper et al., 2014; Cockerill et al., 2017; Kaushal et al., 2019; Galella et al., 2021). Chloride is primarily stored within the saturated zone of riparian floodplains in soils, groundwater, or other subsurface storage (Kelly et al., 2008; Ledford et al., 2016). Groundwater recharge during overbank flood events in the winter promotes the storage of chloride and other ions within the floodplain (Ledford et al., 2016). During low chloride overbank flood events, the salty groundwater is flushed out of

the floodplains and into the stream, acting as a source of salt ions (Ledford et al., 2016; Cockerill et al., 2017). The residence time of these ions can be up to 55 days (Ledford et al., 2016). The retention of salt-laden groundwater in the riparian floodplain would form chemical cocktails with different compositions due to the seasonality, pollutant type, land use or restoration and conservation, and location downstream.

Currently, many salt ions are unregulated and unmanaged; there are no total maximum daily loads (TMDLs) or national primary drinking water regulations (Bhide et al., 2021, 2021; Grant et al., 2022). Without formal regulations, the most common management practice to reduce the concentration of salt ions is to promote retention via restoration and best management practices (BMPs) along flowpaths (Kaushal et al., 2021, 2022a). This study provides a first step towards understanding how FSS is transmitted along watershed flowpaths to sensitive receiving waters, including major drinking water supplies, and identifying benefits and limitations in the role of restoration and conservation in attenuating FSS along flowpaths (Bhide et al., 2021; Grant et al., 2022; Kaushal et al., 2022a, 2022b).

5. Knowledge Gaps and Future Research

Restoration and conservation areas are often implemented for their ability to reduce denitrification and improve stream quality. However, these sites are usually studied on a small scale for a relatively short time period and analyzes only a few elements or nutrients at a time. Here, we studied salt ions, trace metals, and nutrients

across time and space before, during, and after FSS pollution events. By temporally and spatially studying chemical cocktails along restoration and conservation flowpaths, rather than individual contaminants, there can be improvements to pollutant tracking, the co-management of pollutants, the determination of thresholds for contaminant mobilization in response to FSS pollution events, and the development of sensor proxies for harmful pollutants (Trowbridge et al., 2010; Moore et al., 2019; Kaushal et al., 2020; Galella et al., 2021). These methodologies can highlight areas with increased influence of FSS pollution and establish the locations to effectively implement restoration and conservation (Kaushal et al., 2022a).

In recent years, there has been an emphasis on understanding the retention and release of salt ions from stormwater best management practices such as retention ponds, rain gardens, natural or accidental wetlands, and bioswales (Kaushal et al., 2022a). However, less research has focused on stream restoration efforts such as floodplain reconnection to understand if there is retention of salt ions in the floodplain soils during various FSS pollution events. For example, if the concentrations of chemical cocktails decrease downstream of restored stream reaches and floodplains and riparian buffers, these features can be used to manage different types of chemical cocktails in the future.

The chemical cocktail methodology provides a statistical way to assess the sources, transport, and transformation in elemental combinations over space and time (Kaushal et al., 2020). Other studies can use the chemical cocktail approach and can expand the network of data to include a variety of different geographical locations,

pollution events, and locations. This work illustrates how chemical cocktails can be parsed from complex environmental data using PCA. PCA results characterize chemical cocktails in a way that is reproducible. For example, every PCA analysis is associated with a series of reproducible equations. Based on these equations, other studies can compare the chemical cocktails they measure in their own regions of the world to the chemical cocktails we have characterized using the equations. Thus, our approach offers a unique point of comparison for other studies looking to evaluate chemical cocktails in their own systems.

6. Conclusion

Three categories of chemical cocktails formed over space and time: 1) higher concentration of salt ion and trace metals chemical cocktails from road salt events, 2) chemical cocktails lower in salt ions and trace metals during baseflow and stormwater events, and 3) Ca^{2+} and K^{+} enriched chemical cocktails from wastewater effluent. In general, chemical cocktails during baseflow and stormwater events were attenuated downstream over short time scales as streams flowed through restoration and conservation areas. However, road salt events overwhelmed the capacity for restoration and conservation to attenuate chemical cocktails. Few studies have focused on the transport and transformation of salt ions, metals, and nutrients along watershed flowpaths, particularly flowpaths with conservation and restoration. Our results provide further insights on the formation and potential for longitudinal attenuation of chemical cocktails during different pollution events and within reaches

with restoration and conservation. Conservation and restoration can improve downstream water quality associated with different pollution events, but the attenuation capacity of streams, floodplains, and riparian zones can be overwhelmed by freshwater salinization.

Appendices

SI Table 1. Equations were fit to the decline from the peak Na^+ concentrations to the return to the baseflow Na^+ concentration conditions. The best fit type was a second order polynomial. All relationships were significant.

USGS Gauge Site	Fit Type	Equation	R^2	p-value
Anacostia at Bladensburg	Exponential	$y = 2x10^{308}e^{-5.67x}$	0.86	0.0006
Paint Branch	Exponential	$y = 2x10^{308}e^{-5.88x}$	0.77	0.0036
Sligo Creek	Exponential	$y = 2x10^{308}e^{-6.46x}$	0.77	0.0044
Scotts Level Branch	Exponential	$y = 2x10^{308}e^{-5.84x}$	0.71	0.0064

SI Table 2. PCA equations for Figure 5a and Figure 5b. Principal component 1 and principal component 2 will be calculated separately. To calculate the PCA, use the data in the table below and use this formula:
PC1 = ((data-mean)/SD)*PC1 for each ion. Sum all of these together to calculate PC1. Do the same process for PC2.

	Figure 5a				**Figure 5b**			
Ion	*Mean*	*SD*	*PC1*	*PC2*	*Mean*	*SD*	*PC1*	*PC2*
Ba^{2+}	0.18	0.07	-0.02	0.12	0.12	0.069	0.31	0.15
Ca^{2+}	31.0	13.76	0.44	-0.11	43.45	20.65	0.43	-0.26
Cu	0.02	0.03	0.11	0.21	0.039	0.46	0.32	0.040
Fe	0.14	0.10	-0.17	0.53	0.16	0.17	-0.062	0.64
K^+	3.68	1.23	0.41	0.22	4.49	2.99	0.33	-0.31
Mg^{2+}	7.51	3.59	-0.30	-0.21	9.09	6.12	0.32	0.098
Mn	0.04	0.05	0.11	0.60	0.083	0.13	0.23	0.57
Na^+	48.78	59.34	0.32	0.39	84.62	103.37	0.41	0.22
Sr^{2+}	0.16	0.07	0.47	-0.10	0.18	0.092	0.43	-0.14
Tdn	0.96	0.31	0.41	-0.14				

SI Table 3. PCA equations for Figure 6a-6c. Use the equation: ((data – mean)/SD) *PC for all the ions. Calculate PC1 and PC2 separately.

	Ion	Ba^{2+}	Ca^{2+}	Cu	Fe	K^{+}	Mg^{2+}	Mn	Na^{+}	Sr^{2+}
6a: Bull Run	*Mean*	0.091	50.75	0.042	0.087	6.4	6.55	0.039	57.76	0.21
	SD	0.045	15.65	0.036	0.074	3.66	4.12	0.065	48.48	0.057
	PC1	0.49	0.11	0.49	0.23	0.17	0.34	0.11	0.5	0.21
	PC2	-0.084	0.59	-0.10	-0.38	0.45	0.054	-0.34	-0.058	0.41
6b: Rock Creek	*Mean*	0.11	33.42	0.033	0.33	3.5	8.29	0.14	121.58	0.16
	SD	0.036	13.22	0.042	0.13	1.43	3.16	0.098	118.8	0.044
	PC1	0.16	0.3	-0.01	-0.21	0.41	0.38	0.21	0.46	0.46
	PC2	0.22	-0.11	-0.8	0.1	0.28	-0.42	0.16	0.032	0.087
6c: Scotts Level Branch	*Mean*	0.15	43.17	0.044	0.13	3.63	11.96	0.058	88.32	0.17
	SD	0.089	15.86	0.055	0.088	1.93	7.58	0.053	102.98	0.091
	PC1	0.19	0.41	0.4	-0.06	0.39	0.19	0.3	0.41	0.42
	PC2	-0.47	0.002	0.2	0.59	0.19	-0.56	-0.01	0.2	-0.01

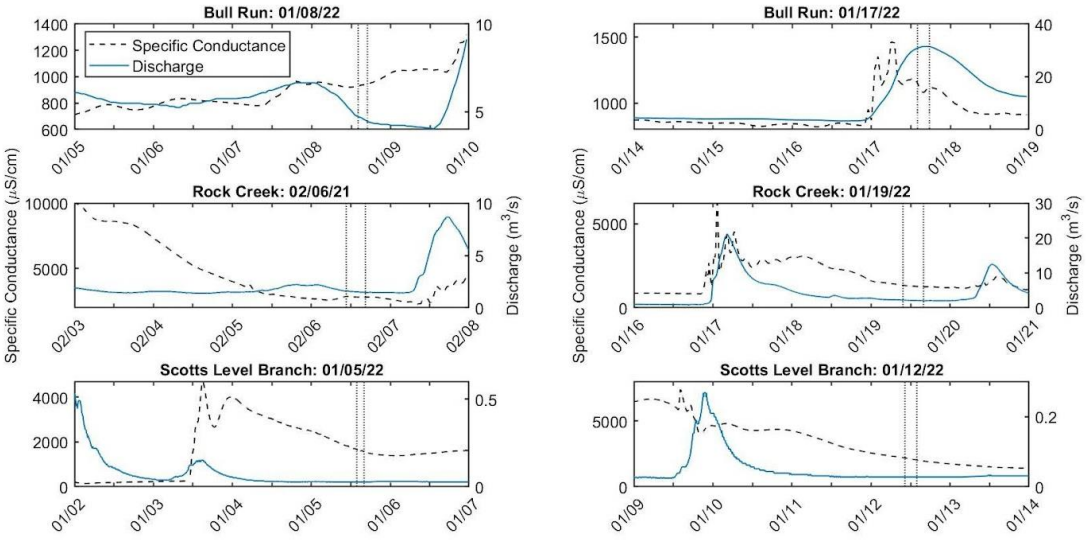

SI Figure 1. Sampling conditions for each of the winter road salt events. Sampling occurred during the dashed vertical lines.

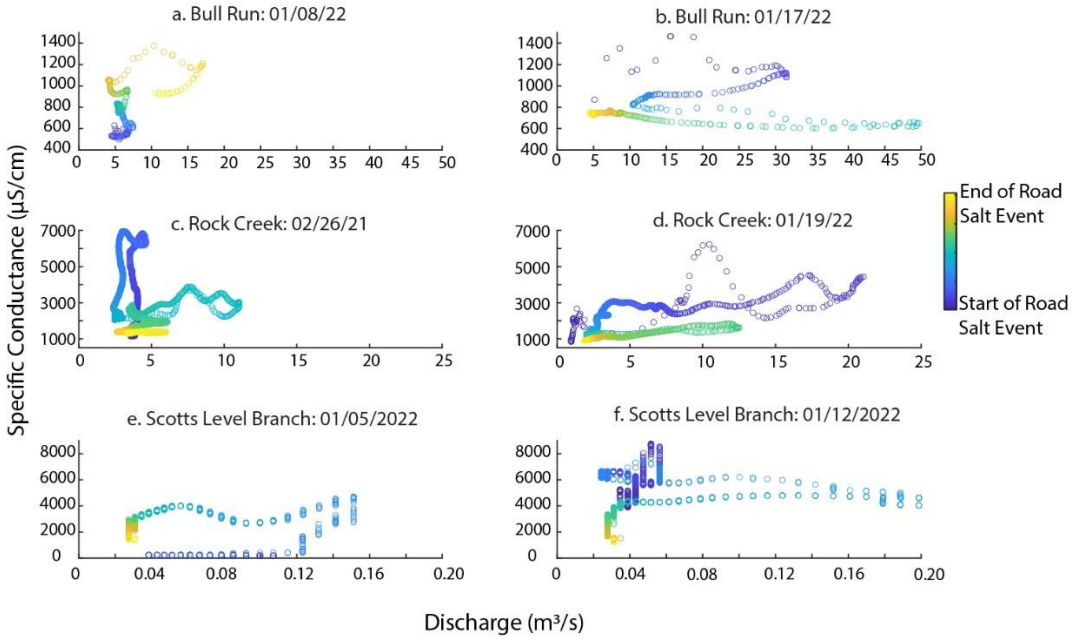

SI Figure 2. Hysteresis loops of discharge and specific conductance from the starting point to the end of the winter road salt events. The data plotted is from the long-term high frequency monitoring stations along t each river. The darker blue circles indicate the start of the road salt event and yellow indicates the end of the road salting events.

Bibliography

Aryal, R., Vigneswaran, S., Kandasamy, J., and Naidu, R. (2010). Urban stormwater quality and treatment. *Korean J. Chem. Eng.* 27, 1343–1359. doi: 10.1007/s11814-010-0387-0.

Azizian, M., Boano, F., Cook, P. L. M., Detwiler, R. L., Rippy, M. A., and Grant, S. B. (2017). Ambient groundwater flow diminishes nitrate processing in the hyporheic zone of streams. *Water Resources Research* 53, 3941–3967. doi: 10.1002/2016WR020048.

Behbahani, A., Ryan, R. J., and McKenzie, E. R. (2021). Impacts of salinity on the dynamics of fine particles and their associated metals during stormwater management. *Science of The Total Environment* 777, 146135. doi: 10.1016/j.scitotenv.2021.146135.

Bernhardt, E. S., Rosi, E. J., and Gessner, M. O. (2017). Synthetic chemicals as agents of global change. *Frontiers in Ecology and the Environment* 15, 84–90. doi: 10.1002/fee.1450.

Bhide, S. V., Grant, S. B., Parker, E. A., Rippy, M. A., Godrej, A. N., Kaushal, S., et al. (2021). Addressing the contribution of indirect potable reuse to inland freshwater salinization. *Nat Sustain*. doi: 10.1038/s41893-021-00713-7.

Bird, D. L., Groffman, P. M., Salice, C. J., and Moore, J. (2018). Steady-State Land Cover but Non-Steady-State Major Ion Chemistry in Urban Streams. *Environ. Sci. Technol.* 52, 13015–13026. doi: 10.1021/acs.est.8b03587.

Blaszczak, J. R., Delesantro, J. M., Zhong, Y., Urban, D. L., and Bernhardt, E. S. (2019). Watershed urban development controls on urban streamwater chemistry variability. *Biogeochemistry* 144, 61–84. doi: 10.1007/s10533-019-00572-7.

Canedo-Arguelles, M., Hawkins, C. P., Kefford, B. J., Schafer, R. B., Dyack, B. J., Brucet, S., et al. (2016). Saving freshwater from salts. *Science* 351, 914–916. doi: 10.1126/science.aad3488.

Castelar, S., Bernal, S., Ribot, M., Merbt, S. N., Tobella, M., Sabater, F., et al. (2022). Wastewater treatment plant effluent inputs influence the temporal variability of nutrient uptake in an intermittent stream. *Urban Ecosyst*. doi: 10.1007/s11252-022-01228-5.

Chen, L., Zhi, X., Shen, Z., Dai, Y., and Aini, G. (2018). Comparison between snowmelt-runoff and rainfall-runoff nonpoint source pollution in a typical urban catchment in Beijing, China. *Environ Sci Pollut Res* 25, 2377–2388. doi: 10.1007/s11356-017-0576-z.

Cintron, N. (2016). Effects of Environmental and Anthropogenic Factors on Water Quality in the Rock Creek Watershed. Uniformed Services University of the Health Sciences Bethesda United States Available at: https://apps.dtic.mil/sti/citations/AD1036472 [Accessed July 1, 2022].

Cockerill, K., Anderson, W. P., Harris, F. C., and Straka, K. (2017). Hot, Salty Water: A Confluence of Issues in Managing Stormwater Runoff for Urban Streams. *JAWRA Journal of the American Water Resources Association* 53, 707–724. doi: https://doi.org/10.1111/1752-1688.12528.

Cooper, C. A., Mayer, P. M., and Faulkner, B. R. (2014). Effects of road salts on groundwater and surface water dynamics of sodium and chloride in an urban restored stream. *Biogeochemistry* 121, 149–166. doi: 10.1007/s10533-014-9968-z.

Crowley, W. P., and Reinhardt, J. (1980). Geologic map of the Ellicott City quadrangle, Maryland. Available at: https://ngmdb.usgs.gov/ngm-bin/pdp/zui_viewer.pl?id=52960 [Accessed June 22, 2022].

Cubas, F. J., Novak, J. T., Godrej, A. N., and Grizzard, T. J. (2014). Effects of Nitrate Input from a Water Reclamation Facility on the Occoquan Reservoir Water Quality. *Water Environment Research* 86, 123–133. doi: 10.2175/106143013X13596524517067.

Dougherty, M., Dymond, R. L., Grizzard, T. J., Godrej, A. N., Zipper, C. E., and Randolph, J. (2007). Quantifying Long-Term Hydrologic Response in an Urbanizing Basin. *J. Hydrol. Eng.* 12, 33–41. doi: 10.1061/(ASCE)1084-0699(2007)12:1(33).

Ekström, S. M., Regnell, O., Reader, H. E., Nilsson, P. A., Löfgren, S., and Kritzberg, E. S. (2016). Increasing concentrations of iron in surface waters as a consequence of reducing conditions in the catchment area. *Journal of Geophysical Research: Biogeosciences* 121, 479–493. doi: 10.1002/2015JG003141.

Findlay, S. E. G., and Kelly, V. R. (2011). Emerging indirect and long-term road salt effects on ecosystems. *Ann N Y Acad Sci* 1223, 58–68. doi: 10.1111/j.1749-6632.2010.05942.x.

Froelich, A. J. (1975). Bedrock map of Montgomery County, Maryland. Available at: https://ngmdb.usgs.gov/ngm-bin/pdp/zui_viewer.pl?id=40354 [Accessed June 22, 2022].

Galella, J. G., Kaushal, S. S., Wood, K. L., Reimer, J. E., and Mayer, P. M. (2021). Sensors track mobilization of `chemical cocktails' in streams impacted by road salts in the Chesapeake Bay watershed. *Environ. Res. Lett.* 16, 035017. doi: 10.1088/1748-9326/abe48f.

Galella, J. G., Kaushal, Sujay S., S. S., Mayer, P. M., Maas, C. M., Shatkay, R. R., and Stutzke, R. A. (Accepted). Stormwater management BMPs: novel sources and sinks of chemical cocktails mobilized by Freshwater Salinization Syndrome. *Frontiers in Environmental Science*.

Glaser, J. D. (2003). Geologic map of Prince George's County, Maryland. Available at: https://ngmdb.usgs.gov/ngm-bin/pdp/zui_viewer.pl?id=52947 [Accessed June 22, 2022].

Grant, S. B., Gomez-Velez, J. D., and Ghisalberti, M. (2018). Modeling the Effects of Turbulence on Hyporheic Exchange and Local-to-Global Nutrient

Processing in Streams. *Water Resources Research* 54, 5883–5889. doi: 10.1029/2018WR023078.
Grant, S. B., Rippy, M. A., Birkland, T. A., Schenk, T., Rowles, K., Misra, S., et al. (2022). Can Common Pool Resource Theory Catalyze Stakeholder-Driven Solutions to the Freshwater Salinization Syndrome? *Environ. Sci. Technol.* 56, 13517–13527. doi: 10.1021/acs.est.2c01555.
Green, S. M., and Cresser, M. S. (2008). Are calcareous soils in uplands less prone to damage from road salting than acidic soils? *Chemistry and Ecology* 24, 1–13. doi: 10.1080/02757540701814614.
Hallberg, M., Renman, G., and Lundbom, T. (2007). Seasonal Variations of Ten Metals in Highway Runoff and their Partition between Dissolved and Particulate Matter. *Water Air Soil Pollut* 181, 183–191. doi: 10.1007/s11270-006-9289-5.
Haq, S., Kaushal, S. S., and Duan, S. (2018). Episodic salinization and freshwater salinization syndrome mobilize base cations, carbon, and nutrients to streams across urban regions. *Biogeochemistry* 141, 463–486. doi: 10.1007/s10533-018-0514-2.
Helena, B., Pardo, R., Vega, M., Barrado, E., Fernandez, J. M., and Fernandez, L. (2000). Temporal evolution of groundwater composition in an alluvial aquifer (Pisuerga River, Spain) by principal component analysis. *Water Research* 34, 807–816. doi: 10.1016/S0043-1354(99)00225-0.
Hemlock Overlook Regional Park (2022). *Wikipedia*. Available at: https://en.wikipedia.org/w/index.php?title=Hemlock_Overlook_Regional_Park&oldid=1078194863 [Accessed November 3, 2022].
Hintz, W. D., Fay, L., and Relyea, R. A. (2022). Road salts, human safety, and the rising salinity of our fresh waters. *Frontiers in Ecology and the Environment* 20, 22–30. doi: 10.1002/fee.2433.
Hu, S., Luo, T., and Jing, C. (2013). Principal component analysis of fluoride geochemistry of groundwater in Shanxi and Inner Mongolia, China. *Journal of Geochemical Exploration* 135, 124–129. doi: 10.1016/j.gexplo.2012.08.013.
Iglesias, M. C.-A. (2020). A review of recent advances and future challenges in freshwater salinization. *Limnetica* 39, 185–211.
Jalali, M., Merikhpour, H., Kaledhonkar, M. J., and Van Der Zee, S. E. A. T. M. (2008). Effects of wastewater irrigation on soil sodicity and nutrient leaching in calcareous soils. *Agricultural Water Management* 95, 143–153. doi: 10.1016/j.agwat.2007.09.010.
Johnny Moore Stream Valley Park *MonsterAttractions*. Available at: https://monsterattractions.com/attractions/places/johnny-moore-stream-valley-park-1195690 [Accessed November 3, 2022].
Kaushal, S., Reimer, J. E., Mayer, P. M., Shatkay, R. R., Maas, C., Nguyen, W. D., et al. (2022a). Freshwater Salinization Syndrome Alters Retention and Release of 'Chemical Cocktails' along Flowpaths: from Stormwater

Management to Urban Streams. *Freshwater Science*, 721469. doi: 10.1086/721469.
Kaushal, S. S. (2016). Increased Salinization Decreases Safe Drinking Water. *Environ. Sci. Technol.* 50, 2765–2766. doi: 10.1021/acs.est.6b00679.
Kaushal, S. S., and Belt, K. T. (2012). The urban watershed continuum: evolving spatial and temporal dimensions. *Urban Ecosyst* 15, 409–435. doi: 10.1007/s11252-012-0226-7.
Kaushal, S. S., Duan, S., Doody, T. R., Haq, S., Smith, R. M., Newcomer Johnson, T. A., et al. (2017). Human-accelerated weathering increases salinization, major ions, and alkalinization in fresh water across land use. *Applied Geochemistry* 83, 121–135. doi: 10.1016/j.apgeochem.2017.02.006.
Kaushal, S. S., Gold, A. J., Bernal, S., Johnson, T. A. N., Addy, K., Burgin, A., et al. (2018a). Watershed 'chemical cocktails': forming novel elemental combinations in Anthropocene fresh waters. *Biogeochemistry* 141, 281–305. doi: 10.1007/s10533-018-0502-6.
Kaushal, S. S., Groffman, P. M., Band, L. E., Shields, C. A., Morgan, R. P., Palmer, M. A., et al. (2008a). Interaction between Urbanization and Climate Variability Amplifies Watershed Nitrate Export in Maryland. *Environ. Sci. Technol.* 42, 5872–5878. doi: 10.1021/es800264f.
Kaushal, S. S., Groffman, P. M., Likens, G. E., Belt, K. T., Stack, W. P., Kelly, V. R., et al. (2005). Increased salinization of fresh water in the northeastern United States. *Proceedings of the National Academy of Sciences* 102, 13517–13520.
Kaushal, S. S., Groffman, P. M., Mayer, P. M., Striz, E., and Gold, A. J. (2008b). Effects of stream restoration on denitrification in an urbanizing watershed. *Ecological Applications* 18, 789–804.
Kaushal, S. S., Likens, G. E., Jaworski, N. A., Pace, M. L., Sides, A. M., Seekell, D., et al. (2010). Rising stream and river temperatures in the United States. *Frontiers in Ecology and the Environment* 8, 461–466. doi: https://doi.org/10.1890/090037.
Kaushal, S. S., Likens, G. E., Pace, M. L., Haq, S., Wood, K. L., Galella, J. G., et al. (2019). Novel 'chemical cocktails' in inland waters are a consequence of the freshwater salinization syndrome. *Phil. Trans. R. Soc. B* 374, 20180017. doi: 10.1098/rstb.2018.0017.
Kaushal, S. S., Likens, G. E., Pace, M. L., Reimer, J. E., Maas, C. M., Galella, J. G., et al. (2021). Freshwater salinization syndrome: from emerging global problem to managing risks. *Biogeochemistry*. doi: 10.1007/s10533-021-00784-w.
Kaushal, S. S., Likens, G. E., Pace, M. L., Utz, R. M., Haq, S., Gorman, J., et al. (2018b). Freshwater salinization syndrome on a continental scale. *PNAS* 115, E574–E583. doi: 10.1073/pnas.1711234115.
Kaushal, S. S., Mayer, P. M., Likens, G. E., Reimer, J. E., Maas, C. M., Rippy, M. A., et al. (2022b). Five state factors control progressive stages of freshwater

salinization syndrome. *Limnology and Oceanography Letters*. doi: 10.1002/lol2.10248.

Kaushal, S. S., Mayer, P. M., Vidon, P. G., Smith, R. M., Pennino, M. J., Newcomer, T. A., et al. (2014). Land Use and Climate Variability Amplify Carbon, Nutrient, and Contaminant Pulses: A Review with Management Implications. *JAWRA Journal of the American Water Resources Association* 50, 585–614. doi: https://doi.org/10.1111/jawr.12204.

Kaushal, S. S., Wood, K. L., Galella, J. G., Gion, A. M., Haq, S., Goodling, P. J., et al. (2020). Making 'chemical cocktails' – Evolution of urban geochemical processes across the periodic table of elements. *Applied Geochemistry* 119, 104632. doi: 10.1016/j.apgeochem.2020.104632.

Kayhanian, M., Fruchtman, B. D., Gulliver, J. S., Montanaro, C., Ranieri, E., and Wuertz, S. (2012). Review of highway runoff characteristics: Comparative analysis and universal implications. *Water Research* 46, 6609–6624. doi: 10.1016/j.watres.2012.07.026.

Kefford, B. J. (2018). Why are mayflies (Ephemeroptera) lost following small increases in salinity? Three conceptual osmophysiological hypotheses. doi: 10.1098/rstb.2018.0021.

Kelly, V. R., Lovett, G. M., Weathers, K. C., Findlay, S. E. G., Strayer, D. L., Burns, D. J., et al. (2008). Long-Term Sodium Chloride Retention in a Rural Watershed: Legacy Effects of Road Salt on Streamwater Concentration. *Environ. Sci. Technol.* 42, 410–415. doi: 10.1021/es071391l.

Lê, S., Josse, J., and Husson, F. (2008). FactoMineR: An R Package for Multivariate Analysis. *Journal of Statistical Software* 25, 1–18. doi: 10.18637/jss.v025.i01.

Ledford, S. H., Lautz, L. K., and Stella, J. C. (2016). Hydrogeologic Processes Impacting Storage, Fate, and Transport of Chloride from Road Salt in Urban Riparian Aquifers. *Environ. Sci. Technol.* 50, 4979–4988. doi: 10.1021/acs.est.6b00402.

Ledford, S. H., Lautz, L. K., Vidon, P. G., and Stella, J. C. (2017). Impact of seasonal changes in stream metabolism on nitrate concentrations in an urban stream. *Biogeochemistry* 133, 317–331. doi: 10.1007/s10533-017-0336-7.

Livesley, S. J., McPherson, E. G., and Calfapietra, C. (2016). The Urban Forest and Ecosystem Services: Impacts on Urban Water, Heat, and Pollution Cycles at the Tree, Street, and City Scale. *Journal of Environmental Quality* 45, 119–124. doi: 10.2134/jeq2015.11.0567.

Lowrance, R., Altier, L. S., Newbold, J. D., Schnabel, R. R., Groffman, P. M., Denver, J. M., et al. (1997). Water quality functions of riparian forest buffers in Chesapeake Bay watersheds. *Environmental Management* 21, 687–712.

Luthy, R. G., Sedlak, D. L., Plumlee, M. H., Austin, D., and Resh, V. H. (2015). Wastewater-effluent-dominated streams as ecosystem-management tools in a drier climate. *Frontiers in Ecology and the Environment* 13, 477–485. doi: 10.1890/150038.

Maas, C. M., Anderson, W. P., and Cockerill, K. (2021). Managing Stormwater by Accident: A Conceptual Study. *Water* 13, 1492. doi: 10.3390/w13111492.

Manassas, M. A. 12521 L. H., and Us, V. 20109 P. 703 361-1339 x0 C. Basic Information - Manassas National Battlefield Park (U.S. National Park Service). Available at: https://www.nps.gov/mana/planyourvisit/basicinfo.htm [Accessed November 3, 2022].

Masoner, J. R., Kolpin, D. W., Cozzarelli, I. M., Barber, L. B., Burden, D. S., Foreman, W. T., et al. (2019). Urban Stormwater: An Overlooked Pathway of Extensive Mixed Contaminants to Surface and Groundwaters in the United States. *Environ. Sci. Technol.* 53, 10070–10081. doi: 10.1021/acs.est.9b02867.

Mayer, P. M., Groffman, P. M., Striz, E. A., and Kaushal, S. S. (2010). Nitrogen Dynamics at the Groundwater–Surface Water Interface of a Degraded Urban Stream. *Journal of Environmental Quality* 39, 810–823. doi: https://doi.org/10.2134/jeq2009.0012.

Mayer, P. M., Reynolds, S. K., McCutchen, M. D., and Canfield, T. J. (2007). Meta-Analysis of Nitrogen Removal in Riparian Buffers. *Journal of Environmental Quality* 36, 1172–1180. doi: https://doi.org/10.2134/jeq2006.0462.

Miller, C. V., Chanat, J. G., and Bell, J. M. (2013). Water Quality in the Anacostia River, Maryland and Rock Creek, Washington, D.C.: Continuous and Discrete Monitoring with Simulations to Estimate Concentrations and Yields of Nutrients, Suspended Sediment, and Bacteria.

Montgomery Parks (2022). Rock Creek Regional Park. Available at: https://montgomeryparks.org/parks-and-trails/rock-creek-regional-park/ [Accessed July 31, 2022].

Moore, J., Bird, D. L., Dobbis, S. K., and Woodward, G. (2017). Nonpoint Source Contributions Drive Elevated Major Ion and Dissolved Inorganic Carbon Concentrations in Urban Watersheds. *Environ. Sci. Technol. Lett.* 4, 198–204. doi: 10.1021/acs.estlett.7b00096.

Moore, J., Fanelli, R. M., and Sekellick, A. J. (2019). High-frequency data reveal deicing salts drive elevated specific conductance and chloride along with pervasive and frequent exceedances of the US Environmental Protection Agency aquatic life criteria for chloride in urban streams. *Environmental Science & Technology* 54, 778–789.

Morel, C. J., Kaushal, S. S., Tan, M. L., and Belt, K. T. (2020). Developing Sensor Proxies for "Chemical Cocktails" of Trace Metals in Urban Streams. *Water* 12, 2864.

Mulholland, P. J., Helton, A. M., Poole, G. C., Hall, R. O., Hamilton, S. K., Peterson, B. J., et al. (2008). Stream denitrification across biomes and its response to anthropogenic nitrate loading. *Nature* 452, 202–205. doi: 10.1038/nature06686.

National Parks Service (2022). Rock Creek Park (U.S. National Park Service). *National Parks Service*. Available at: https://www.nps.gov/rocr/index.htm [Accessed July 31, 2022].

Northern Virginia Regional Park Authority (2022). Bull Run Regional Park. *Northern Virginia Regional Park Authority*. Available at: https://www.novaparks.com/parks/bull-run-regional-park [Accessed July 31, 2022].

Novotny, V., Muehring, D., Zitomer, D. H., Smith, D. W., and Facey, R. (1998). Cyanide and metal pollution by urban snowmelt: Impact of deicing compounds. *Water Science and Technology* 38, 223–230. doi: 10.1016/S0273-1223(98)00753-7.

Nowak, D. J. (2006). Institutionalizing urban forestry as a "biotechnology" to improve environmental quality. *Urban Forestry & Urban Greening* 5, 93–100. doi: 10.1016/j.ufug.2006.04.002.

Onyango, L., Leslie, G., and Wood, J. G. (2014). Global Potable Reuse Case Study 2: Upper Occoquan Service Authority. Brisbane, Australia: Australian Water Recycling Centre of Excellance.

Ouyang, Y. (2005). Evaluation of river water quality monitoring stations by principal component analysis. *Water Research* 39, 2621–2635. doi: 10.1016/j.watres.2005.04.024.

Peres-Neto, P. R., Jackson, D. A., and Somers, K. M. (2005). How many principal components? stopping rules for determining the number of non-trivial axes revisited. *Computational Statistics & Data Analysis* 49, 974–997. doi: 10.1016/j.csda.2004.06.015.

Pieper, K. J., Tang, M., Jones, C. N., Weiss, S., Greene, A., Mohsin, H., et al. (2018). Impact of Road Salt on Drinking Water Quality and Infrastructure Corrosion in Private Wells. *Environ. Sci. Technol.* 52, 14078–14087. doi: 10.1021/acs.est.8b04709.

Ribot, M., Martí, E., Schiller, D. von, Sabater, F., Daims, H., and Battin, T. J. (2012). Nitrogen processing and the role of epilithic biofilms downstream of a wastewater treatment plant. *Freshwater Science*. doi: 10.1899/11-161.1.

Rice, J., and Westerhoff, P. (2017). High levels of endocrine pollutants in US streams during low flow due to insufficient wastewater dilution. *Nature Geosci* 10, 587–591. doi: 10.1038/ngeo2984.

Rippy, M. A., Deletic, A., Black, J., Aryal, R., Lampard, J.-L., Tang, J. Y.-M., et al. (2017). Pesticide occurrence and spatio-temporal variability in urban run-off across Australia. *Water Research* 115, 245–255. doi: 10.1016/j.watres.2017.03.010.

Rodriguez, C., Van Buynder, P., Lugg, R., Blair, P., Devine, B., Cook, A., et al. (2009). Indirect Potable Reuse: A Sustainable Water Supply Alternative. *International Journal of Environmental Research and Public Health* 6, 1174–1203. doi: 10.3390/ijerph6031174.

Rose, S. (2007). The effects of urbanization on the hydrochemistry of base flow within the Chattahoochee River Basin (Georgia, USA). *Journal of Hydrology* 341, 42–54. doi: 10.1016/j.jhydrol.2007.04.019.

Schulz, C.-J., and Cañedo-Argüelles, M. (2019). Lost in translation: the German literature on freshwater salinization. *Phil. Trans. R. Soc. B* 374, 20180007. doi: 10.1098/rstb.2018.0007.

Scotts Level Branch Stream Restoration Project (2019). Youtube Available at: youtube.com/watch?v=ix42pr9t3ts.

Sellers, A. (2014). Certificate of Analysis.

Shimadzu (2011). Total Organic Carbon Analyzer Manual.

Snodgrass, J. W., Moore, J., Lev, S. M., Casey, R. E., Ownby, D. R., Flora, R. F., et al. (2017). Influence of Modern Stormwater Management Practices on Transport of Road Salt to Surface Waters. *Environ. Sci. Technol.* 51, 4165–4172. doi: 10.1021/acs.est.6b03107.

Stranko, S. A., Hilderbrand, R. H., and Palmer, M. A. (2012). Comparing the Fish and Benthic Macroinvertebrate Diversity of Restored Urban Streams to Reference Streams. *Restoration Ecology* 20, 747–755. doi: 10.1111/j.1526-100X.2011.00824.x.

Sweeney, B. W., Bott, T. L., Jackson, J. K., Kaplan, L. A., Newbold, J. D., Standley, L. J., et al. (2004). Riparian deforestation, stream narrowing, and loss of stream ecosystem services. *Proceedings of the National Academy of Sciences* 101, 14132–14137.

Szklarek, S., Górecka, A., and Wojtal-Frankiewicz, A. (2022). The effects of road salt on freshwater ecosystems and solutions for mitigating chloride pollution - A review. *Science of The Total Environment* 805, 150289. doi: 10.1016/j.scitotenv.2021.150289.

Tomer, M. D., Dosskey, M. G., Burkart, M. R., James, D. E., Helmers, M. J., and Eisenhauer, D. E. (2009). Methods to prioritize placement of riparian buffers for improved water quality. *Agroforest Syst* 75, 17–25. doi: 10.1007/s10457-008-9134-5.

Trowbridge, P. R., Kahl, J. S., Sassan, D. A., Heath, D. L., and Walsh, E. M. (2010). Relating Road Salt to Exceedances of the Water Quality Standard for Chloride in New Hampshire Streams. *Environ. Sci. Technol.* 44, 4903–4909. doi: 10.1021/es100325j.

U. S. Geological Survey (2016). USGS Water Data for the Nation. Available at: https://waterdata.usgs.gov/nwis [Accessed August 4, 2022].

Upper Occoquan Service Authority (2022). Available at: https://uosa.org/history/ [Accessed November 1, 2022].

Utz, R., Bidlack, S., Fisher, B., and Kaushal, S. (2022). Urbanization drives geographically heterogeneous freshwater salinization in the northeastern United States. *Journal of Environmental Quality* 51, 952–965. doi: 10.1002/jeq2.20379.

Velinsky, D. J., Riedel, G. F., Ashley, J. T. F., and Cornwell, J. C. (2011). Historical contamination of the Anacostia River, Washington, D.C. *Environ Monit Assess* 183, 307–328. doi: 10.1007/s10661-011-1923-z.

Vidon, P., Allan, C., Burns, D., Duval, T. P., Gurwick, N., Inamdar, S., et al. (2010). Hot Spots and Hot Moments in Riparian Zones: Potential for Improved Water Quality Management. *JAWRA Journal of the American Water Resources Association* 46, 278–298. doi: 10.1111/j.1752-1688.2010.00420.x.

Wood, K. L., Kaushal, S. S., Vidon, P. G., Mayer, P. M., and Galella, J. G. (2022). Tree trade-offs in stream restoration: impacts on riparian groundwater quality. *Urban Ecosyst* 25, 773–795. doi: 10.1007/s11252-021-01182-8.